Third International Conference on Inverse Design Concepts and Optimization in Engineering Sciences (ICIDES-III), Editor G.S. Dulikravich, Washington D.C. October 23-25, 1991.

REVIEW OF AERODYNAMIC DESIGN IN THE NETHERLANDS

by

Th.E.Labrujère

National Aerospace Laboratory NLR
Anthony Fokkerweg 2
1059 CM AMSTERDAM
THE NETHERLANDS

SUMMARY

A survey is given of aerodynamic design activities in The Netherlands, which take place mainly at Fokker, NLR and Delft University of Technology (TUD). The survey concentrates on the development of the Fokker 100 wing, glider design at TUD and research at NLR in the field of aerodynamic design. Results are shown to illustrate these activities.

1.INTRODUCTION

In the Netherlands, activities in the field of aerodynamic design take place at the aircraft factory Fokker, the aeronautical research institute NLR and the Technical University of Delft.

A well known product of these activities is the civil transport aircraft Fokker 100 (See fig.1.1). But no less successful is the ASW-24 glider designed by Boermans at the Low Speed Laboratory of TUD in collaboration with Alexander Segelflugzeugbau in Germany(See Fig.1.2).

Very often, new aircrafts result from modifying existing aircraft, aiming at e.g. improvement of performance, adaption to changed market requirements or improvement of economics in view of operating environment. In that way, the Fokker 100 has been derived from the Fokker F28 (see Fig.1.3) by means of sometimes drastic modifications. Also, the gliders designed at Delft are the result of continuous attempts to reach the limits of sailplane performance.

These developments would not have been possible without the help of computational tools which play an essential role in both the actual design process and the analysis of wind tunnel measurements and also at the interpretation of flight test data.

The present paper deals with the main aerodynamic design objectives pursued at the development of the transport aircraft Fokker 100 and the glider ASW-24 and the process followed to attain them. In conclusion, special attention will be paid to research activities at NLR in the field of computational fluid dynamics in support of design developments.

2.THE FOKKER 100.

The Fokker 100 design will be illustrated by considering two of the main design problems solved during development. A more complete and detailed account can be found in Refs. 1 and 2.

The Fokker 100 wing has been derived from the F-28 wing, which is determined by four wing sections connected with straight generators. The main objective for a new wing design was improvement of the Mach drag rise characteristics. The F-28 was originally designed for a lift coefficient of C_L=0.2 whereas the new design requirements lead to a C_L=0.4 to 0.5 at which condition the transonic drag increase of the F-28 wing is not negligible.

Third International Conference on Inverse Design Concepts and Optimization in Engineering Sciences
(ICIDES-III), Editor: G.S. Dulikravich, Washington D.C., October 23-25, 1991.

Table I presents a survey of the most important modifications that have been implemented successively, thus defining a number of new wing shapes which have been analyzed by means of both computations and wind tunnel measurements.

The modifications applied to wing sections I and II in wing 4 resulted from a computational study with the help of a viscous transonic flow code, which predicted a significant improvement of the Mach drag rise characteristics as a consequence of these modifications (See Fig.2.1). This was fully confirmed by means of wind tunnel measurements, though it appeared necessary to improve the stalling characteristics of the outer wing.

Computational analysis led to the conclusion that the Mach drag rise characteristics could be improved by a further modification of section I. Moreover, by modifying section IV improvement of the outer wing stall behaviour was expected. Test results for the thus defined wings 5 and 6 are presented in Fig.2.2 indicating a further improvement when compared with wings 3 and 4.

As a preliminary final step wing 8 was defined, combining a rearward chord extension with rear camber. This modification led to a second improvement of the drag rise characteristics as illustrated by Fig.2.3 for section II.

At that time, however, it appeared necessary to adapt the design goals to market requirements in terms of an increase of take-off weight. This led to the definition of wing 10, which happened to exhibit a rather large drag rise at low lift coefficients cruising conditions. Subsequent reduction led to the definition of wing 11 (See Fig.2.4).

Modification of the lower leading edge of sections II and IV resulted in wing 11. The effect of this modification is shown in Figs. 2.4 and 2.5. And, finally, modification of section II leading to the definition of wing 12 took care of the design requirement with respect to the stalling behaviour.

In conclusion, a survey of the main modifications applied to the original F-28 wing is given by means of Fig.2.6 where a comparison is made between the definitive wing planform for the Fokker 100 and the F-28 wing planform and where also the basic wing sections are compared. This figure shows that a large part of the original F-28 wing has still been retained. The main differences are the span extension and leading as well as trailing edge modifications. However, as has been verified by means of wind tunnel measurements these modifications were sufficient for attaining amongst other things the design goals with respect to high- and low speed drag, buffet onset boundary and stalling behaviour.
Another important design problem was the improvement of the stub wing with respect to its drag characteristics. At the new cruising conditions the flow around the original F-28 stub wing contained regions with supersonic velocities, thus leading to undesirable wave drag. It appeared to be possible to reshape the stub wing such that the flow remained subcritical over the entire range of cruise lift coefficients.

Finally, some attention may be paid to the computer codes used during the design process. A major role has been played by two transonic flow analysis codes i.e. the 3D code XFLO-22 and a 2D viscous transonic flow code by means of which the effect of the various wing modifications was predicted. The wing modifications were based on earlier wing design computations, preceding the actual Fokker 100 wing design, by means of the constrained inverse code for the design of wings with a given pressure distribution in subsonic flow of Ref.3. More recently this code has been extended for application to supercritical flow conditions (Ref.4).

Third International Conference on Inverse Design Concepts and Optimization in Engineering Sciences
(ICIDES-III), Editor G.S. Dulikravich, Washington D.C., October 23-25, 1991.

The wing design system is based on an inverse method of the residual correction type, combining a direct flow solver for transonic flow with simple geometric correction rules. In order to fulfil requirements from the structural engineer's point of view, geometric constraints are taken into account.

The transonic wing-body code XFLO-22 (Ref.6) is an extension of the non-conservative finite difference wing code FLO-22 (Ref.5) of Jameson and Caughey modified to simulate fuselage cross-flow effects. This simulation is achieved by replacing the boundary condition of zero normal velocity in the plane of symmetry in the original code by a condition of prescribed non-zero normal velocity, the latter being computed by means of the NLR panel method (Ref.7,8). By means of post-processing viscous effects may then be estimated using the 3-D laminar/turbulent boundary layer code BOLA (Ref.9).

An example of the usefulness of XFLO-22 is given in Fig.2.7 where a comparison is made between calculated and measured (wind tunnel and flight test) pressure distributions for two wing stations. It may be noted that a surprisingly good correlation is shown. Presumably the applied condition of taking the trailing edge flow tangential to the lower wing surface, when using a grid of 160 (chord) x 32 (span) x 28 (normal) points, compensates for the absence of viscous effects. The same kind of correlation is demonstrated in Fig. 2.8 where a comparison is made between measured and predicted buffet onset boundaries.

For the design problem associated with the stub wing with its strong interaction with the fuselage and the engine nacelle a design code was not available. The problem was solved by combining results of the 2D analogue of the wing design code with 3D panel method calculations (Ref.7). The success of this approach may be illustrated by means of Fig.2.9 where a comparison is made between calculated and measured stub wing pressures.

3.THE SAILPLANE ASW-24

The ASW-24 is a Standard Class Sailplane built by Alexander Schleicher Flugzeugbau in Germany. The aerodynamic design of this glider was performed in close cooperation between the manufacturer and the Low Speed Laboratory (LSL) of Delft University of Technology (TUD). Detailed account of aerodynamic as well as structural design is given in Ref.10.

When designing a glider, the main objectives are maximizing the glide ratio at the higher flight speeds and minimizing the rate of sink at the lower flight speeds. The higher flight speeds are applied when flying from one thermal to another, and the lower flight speeds are used when climbing in a thermal.

A typical glider flight performance polar is shown in Fig.3.1 for the ASW-24. It results from flight test measurements and computational analysis with respect to its component parts. From this figure it appears that the wing contributes considerably to the drag, at higher flight speeds especially in consequence of the profile drag. Accordingly, the history of glider design shows a continuous search for low drag wing profiles, mainly by attempting to maximize the laminar flow region on the airfoils.

When designing airfoils for laminar flow with a view to practical application the key problem is to avoid the appearance of laminar separation bubbles. These bubbles cause pressure drag and have a detrimental effect on the subsequent turbulent boundary layer such that a considerable drag increase results. Thus, the design should be such that transition to turbulent flow occurs before the laminar flow will separate.

Third International Conference on Inverse Design Concepts and Optimization in Engineering Sciences
(ICIDES-III), Editor: G.S. Dulikravich, Washington D.C., October 23-25, 1991

There are a few alternatives to solve this problem. One of these is Wortmann's destabilizing region concept, the other is the application of some tripping device in order to provoke transition to turbulent flow.

When following the destabilizing region concept the airfoil is shaped such that in the region where laminar separation is expected to occur, a slightly adverse pressure gradient is induced. This adverse gradient destabilizes the laminar boundary layer causing transition and thus avoiding flow separation. Application of a tripping device amounts to disturbing the boundary layer by means of artificial roughness on the airfoil surface or by means of blowing.

Both alternatives have been used at the design of the airfoil DU84-158 applied in the ASW-24. The destabilizing region concept has been applied at the upper surface and a tripping device in the form of a so-called "zig-zag tape" has been applied at 77% chord position at the lower surface. The measured pressure distribution of Fig.3.2. shows a laminar separation bubble on the lower surface at about 85% chord and its removal due to application of the zig-zag tape. Transition to turbulent flow on the upper surface is triggered by the adverse gradient at about 59% chord.

The effectiveness of the zig-zag tape is also shown in Fig.3.3 where measured aerodynamic characteristics are given both for the clean airfoil and the taped airfoil. The maximum lift is hardly influenced by the roughness, the stalling behaviour is gentle and the drag reduction is considerable.

As is shown in Fig.3.1, at low speed climbing conditions, more than 50% of the total drag is due to induced drag. So, it will be clear that reduction of induced drag will be another major goal when designing sailplanes; wing planform and aspect ratio being the main parameters when optimizing for induced drag at a given wing loading.

In the present case the wing planform has been chosen with the help of numerical optimization studies based on lifting line theory with taper ratio and spanwise position of taper ratio change as design variables. The aspect ratio has been chosen in combination with the wing loading on the basis of cross country speed optimization studies, for details of which the reader is referred to ref.10.

A third aspect of wing design that may be considered here, is the effect of wing fuselage interaction. Applying the panel method of Ref.7 with the panel schematization of Fig.3.4 the pressure distribution on the wing-fuselage combination has been studied. Fig.3.5 shows the pressure distribution in a few wing sections for two different angles of attack.

The typical modern glider fuselage has been designed such that the forebody fits into the streamlines of the wing at higher lift coefficients in order to avoid the occurrence of high suction peaks in sections near the fuselage (Fig.3.5a). This has, however, as a consequence that at high speed conditions (lower lift coefficient) the cross flow effect is increased (Fig.3.5b), which causes the wing sections close to the fuselage to operate in non-optimal conditions. To improve the flow conditions at the junction of the ASW-24, a small fairing with 7% chord extension has been applied where the wing is lofted towards a wing root airfoil suitable for turbulent flow conditions. Nevertheless, improvement of the wing fuselage junction is still the subject of continuing study.

In the past decades considerable progress in glider design has been made. This may be illustrated by means of Fig.3.6, where the flight performance polar for the present design is shown in comparison with that of two predecessors. The difference in performance is a consequence of the improvement of the aerodynamic

characteristics as illustrated by Fig.3.7 which is mainly due to the wing profiles that have been applied.

In conclusion these profiles may be compared by means of Figs.3.8a,b,c , where calculated inviscid pressure distributions are shown. From these pressure distributions a rough estimate of the laminar flow region can be made, clearly showing the backward displacement of the transition point resulting in a decrease of the drag.

The DU84-158 airfoil has been designed with the help of the LSL computer program for airfoil analysis and design (Refs.12,13). This program is based on Timman's conformal mapping method for inviscid flow (Ref.14) in combination with Thwaites method for laminar and Green's method for turbulent boundary layer flow and the Van Ingen e^9-method for prediction of transition (Ref.15).

4.DEVELOPMENTS AT NLR

In support of aerodynamic aircraft design NLR has a continuing research program for the development of CFD codes both for analysis and design. Gradually, as will have become clear from the preceding sections the tools thus developed are incorporated in the actual design processes followed in the industry. In the present section, some attention will be paid to capabilities that have not yet been (fully) utilized for practical applications. Also, further contributions of NLR to improvement of airfoil- and wing design will be considered.

4.1 AIRFOILS

For analysis and design of airfoils in both subsonic and transonic flow taking viscous effects into account, the MAD computer program system has been developed. On the ICIDES conference of 1984 Slooff has given a global description of the system as it was available at that time (Ref.16).

Since then the system of Ref.17 has been extended by incorporating the transonic design method of Ref.25 in combination with the transonic analysis method of Refs.5 and 6. The general approach followed to solve the design problem has remained the same. It is of the residual correction type where the actual design problem is translated into an equivalent design problem of reduced complexity, thus enabling the application of relatively simple inverse methods and it leads to an iterative design process as depicted in Fig.4.1.
It is assumed that the design goal is formulated in terms of a target pressure distribution and that an initial guess of the airfoil shape will be given. A direct flow solver for either subsonic or transonic viscous flow is used for the determination of the pressure distribution on the gi en airfoil, and a constrained inverse method is used to determine the possibl required modification.

An example of application to a subsonic design problem is described in Refs.19 and 20.
It concerns the improvement with respect to drag behaviour of the wing-slat configuration of Fig.4.2. As becomes clear from Fig.4.3 it has been found in wind tunnel measurements that the flow around this airfoil shows early boundary layer separation on the main wing upper surface at the take-off condition lift coefficient $C_l \approx 2.1$.

With the aid of the method of Ref.18 for the determination of viscous subsonic flow around multi-element airfoils analysis calculations were made. From this analysis it was concluded that reduction of the drag should be attempted by

Third International Conference on Inverse Design Concepts and Optimization in Engineering Sciences
(ICIDES-III), Editor: G.S. Dulikravich, Washington D.C., October 23-25, 1991.

reducing the extent of the separation region. This implied that the adverse pressure gradient on the wing upper surface had to be reduced.

As the basic airfoil geometry should not be altered when designing a wing-slat configuration, the sole possibility to reduce the pressure gradient is to lower the suction peak level on the wing nose, without however reducing the lift coefficient at the same time.

These considerations led to specification of the target as depicted in Fig.4.4, in terms of an equivalent potential flow pressure distribution. The main points of interest are :
(i) a decreased velocity peak on the main wing upper surface aiming at a delay of boundary layer separation,
(ii) increase of expansion around the wing nose aiming at an increase of the slat dumping velocity,
(iii) an increase of the slat dumping velocity aiming at increase of the slat lift contribution,
(iv) an increase of the slat lower surface pressure level aiming at increase of the slat lift and decrease of the slat drag.

Application of the design process depicted in Fig.4.1. led to the result depicted in Fig.4.5. The most striking geometry modification is the blunt nose of the main wing resulting in a rather thin slat trailing edge. Application of the viscous flow analysis method of Ref.18 to the new geometry produced the pressure distribution shown in Fig.4.6 in comparison with that on the original configuration.

Clearly two of the design goals have been attained according two these calculations. The suction peak on the main wing has been reduced and the dumping velocity on the slat has been increased. Hardly visible is a slightly rearward shift of the boundary layer separation point on the wing upper surface (it amounts to about 2% of the local chord) and the pressure level at the slat lower side has decreased instead of increased.

However, as the analysis method has not been developed for the treatment of separated flow regions, the quantitative value of these results is questionable. Moreover the results for the slat lower surface, modelled as shown in Fig.4.1 to simulate the existence of the separation bubble, are of course less reliable. Therefore it was concluded that the results were sufficiently encouraging in order to test the new slat geometry in the wind tunnel.

The measured C_l-α curves for both the original and new configuration are compared in Fig.4.7. Apparently $C_{l_{max}}$ has been retained and the increase of the C_l-α slope indicates reduced viscous losses. This is confirmed by the C_l-C_d curves shown in Fig.4.8 which also shows that at the present design condition ($C_l \approx 2.1$) a drag reduction of more than 30 % has been realized.

Another example of application of the MAD system will be presented in Ref.21. It concerns the design of a medium speed laminar flow airfoil. As a first step in the design process a target pressure distribution was specified. Here the goal was to choose a pressure distribution such that at the upper side the boundary layer would remain laminar over at least 60% of the chord.

The pressure distribution prescribed as target for the upper side of the airfoil is shown in Fig.4.9 together with calculated Re_θ (Reynolds number based on momentum loss thickness). Re_{θ_1} represents the Tollmien-Schlichting stability criterium and Re_{θ_2} is the transition criterium according to Granville. The

Third International Conference on Inverse Design Concepts and Optimization in Engineering Sciences
(ICIDES-III), Editor: G.S. Dulikravich, Washington D.C., October 23-25, 1991

calculations predict instability of the boundary layer for x/c > .14, but a reasonable margin with respect to transition to turbulent flow is left until x/c=.6. As a result of applying the MAD system, an airfoil was obtained which produces the desired pressure distribution perfectly, as is shown in Fig.4.10.

From this example where, in connection with the laminar flow, special attention had to be paid to the nose shape, it has been learned once again, that care has to be given to the leading and trailing edge regions (adaptation of the target without adapting the design goals) in order to obtain convergence and in order to produce realistic airfoil shapes.

Notwithstanding these difficulties the design was successful as may be illustrated by means of Figs.4.11 and 4.12, where a comparison is made between pressure distributions and C_l-C_d curves as measured in the wind tunnel and as calculated by means of VGK, a 2D viscous transonic airfoil code (Ref.23,24), which is an extension of the semi-conservative finite difference method of Garabedian and Korn for inviscid transonic flow, weakly coupled with a boundary layer code based on Thwaites method for laminar and Green's lag-entrainment method for turbulent flow.

To conclude this subsection an application to wind turbine design may be considered (Ref.22). The objective was to design an airfoil with an increased maximum lift over drag ratio. Starting point was a blade based on the NACA 4421 airfoil of which the stall behaviour was considered appropriate for control by stall. Thus the airfoil design had to be done under the side condition that the stall behaviour should remain approximately the same. Moreover, from structural point of view, the thickness over chord ratio had to be at least 0.2.

An existing airfoil which could have been considered for application is the Wortmann FX 84-W-218 airfoil because of its favourable lift over drag ratio. It has, however, an unacceptable stall behaviour. Therefore it was concluded that an airfoil should be designed combining the advantages of both the NACA 4421 and the Wortmann airfoils.

Using CADOS (see section 4.3), a NACA 4421 pressure distribution has been modified in order to specify a target pressure distribution for the MAD system (see Fig.4.13). The target pressure distribution should lead to a flow with a laminar boundary layer in a larger region than at the NACA 4421 airfoil. On the other hand the target laminar flow region is smaller than at the Wortmann airfoil in order to avoid rash stall behaviour.

Application of the MAD system led to the NLR/VSH 8801 airfoil. This airfoil produces the desired pressure distribution as is shown in Fig.4.14. The geometry of the new airfoil is compared with those of the NACA airfoil and the Wortmann airfoil in Fig.4.15. A comparison of the aerodynamic characteristics is made in Fig. 4.16 which presents the calculated lift and moment coefficient as function of the angle of attack and in Fig.4.17 which presents the C_l-C_d curves.

The new airfoil has a somewhat larger lift coefficient than the NACA airfoil. The stall behaviour of both airfoils is approximately the same. For stall controlled wind turbines a lift curve such as that of the Wortmann airfoil with hardly any variation near stall is not useful. The maximum lift over drag ratio of the new airfoil is higher than those of the other airfoils. From these results it has been concluded that the design goal i.e. combination of the advantages of both reference airfoils has been met.

Third International Conference on Inverse Design Concepts and Optimization in Engineering Sciences
(ICIDES-III), Editor: G.S. Dulikravich, Washington D.C., October 23-25, 1991

4.2 WINGS

Since the thin wing inverse panel method for design of wings in subsonic flow became available at NLR in 1974, further developments have gradually increased NLR's capabilities for wing design. To start with, the inverse method was incorporated in the design system (Ref.3) for wings in subsonic flow, using the inverse method for the determination of geometry corrections and the NLR panel method (Ref.7) for analysis of the modified wings. Subsequently, this system was extended for application to transonic flow using the XFLO-22 code of Ref.6 for analysis and applying a 3D analogue of the defect pressure splitting technique of Refs.25,26 for adaptation of the geometry correction procedure to transonic flow (Ref.27).

The practical applicability of the latter transonic wing design system may be demonstrated by means of a reconstruction example presented in Figs.4.18,4.19. Starting point is the well-known DFVLR-F4 wing for the present purpose attached to a simple cylindrical body. The target pressure distribution represented by the dashed line in Fig.4.19a is the pressure distribution as obtained by applying XFLO-22 to the original F4/body geometry of Fig.4.18. An "initial guess" of the geometry which is required at the start of the design process has been obtained by distorting the original geometry. The pressure distribution represented by the lines marked a is produced by this distorted configuration.

Application of the wing design system resulted after 6 iterations in the geometry shown in Fig.4.19b in comparison with the original F4 wing geometry (target). The corresponding pressure distribution is represented by the lines marked b in Fig.4.19a. The target pressure distribution is reproduced near the tip. In the other sections some deviations are still present, especially in the shock region. But the overall agreement between final- and target pressure distribution is satisfactory.

Fig.4.20 presents a functional breakdown of the algorithm. It follows the residual correction approach in which the basic idea is to apply a simple fast geometry correction procedure for determining estimates of the geometry to be designed and an accurate method for analysis of the flow around the current geometry.

In the present version of the design system flow analysis is performed by means of XFLO-22 (Ref.6), a program system based on a combination of Jameson's code FLO-22 (Ref.5) and the NLR panel method (Ref.7). With the aid of the latter method it has been attempted to remove the limitation of FLO-22 to wing-alone configurations. The usefulness of this method for engineering purposes has been demonstrated and validated by comparison with results of wind tunnel tests for a number of wing-body configurations (see Ref.6).

However, it was felt necessary to improve the accuracy of the design system by improving the accuracy of the analysis method , at the same time removing the limitation to wing-alone in a more fundamental way. Therefore, it was decided to develop a new code for transonic flow analysis. This Multi-component Aircraft Transonic Inviscid Computation System (MATRICS) is based on full potential theory applying discretizations according to the finite volume concept (Refs.28,29). It is applicable to wing-body configurations.

The next step in the development of a new analysis code will be the coupling of MATRICS to a boundary layer calculation method in a (strong) interactive way. The subsequent incorporation of that code in the wing design system will be one of the steps towards the development of a system (WINGDES) for the design of wings in viscous transonic flow.

Third International Conference on Inverse Design Concepts and Optimization in Engineering Sciences (ICIDES-III), Editor: G.S. Dulikravich, Washington D.C., October 23-25, 1991

The geometry correction procedure, for which a functional breakdown is given in Fig.4.21, consists of two major steps. From the pressure defect i.e. the difference between the target and the current pressure distribution, an equivalent subsonic perturbation velocity distribution is derived using the splitting technique of Ref.25, whereupon by means of an inverse panel method geometry corrections are determined.

The pressure splitting technique applied to the pressure distribution in a wing section distinguishes between regions with a subsonic and regions with a supersonic flow behaviour. To this end a "critical" pressure coefficient is defined and the assumption is made that subsonic theory should be applied in regions where both target and current pressure distribution are "subcritical" and supersonic theory if both pressure distributions are "supercritical". (see Fig.4.22). Application of subsonic thin wing theory then translates the subsonic pressure defect into subsonic perturbation velocities. Application of supersonic wavy wall formulae leads to translation of the supersonic pressure defect into geometric slope corrections which however, for the sake of similarity in representation, are expressed in equivalent subsonic perturbation velocities by means of thin airfoil analysis.

Some details of the constrained inverse panel method which is applied for the derivation of the geometry corrections from the equivalent perturbation velocities, are given in Fig.4.23. It is essentially a linearized panel method which utilizes on the mean wing plane a distribution of x-doublets for representation of thickness effects and a distribution of vorticity for representation of camber effects and on the body surface constant source panels. Geometry constraints may be applied in the form of prescribed values of thickness and/or camber weighted in order to create a desired balance. The associated over-determined system of equations is solved in a least square error sense. By adding the squares of the residuals associated with the pressure defects and the constraints, each multiplied with their specified weight factors a functional is formed, from which by formal differentiation a new set of equations is derived that is solved by a block iteration procedure.

The geometry correction procedure thus described is very fast as a consequence of which the computing time needed for one iteration step is only slightly more than for one analysis run, however in the leading edge region the thin wing approximation to the real flow is not applicable and leads to difficulties when leading edge modifications are pursued.

4.3.TARGET PRESSURE DISTRIBUTIONS

Many design methods, amongst them the residual correction methods of NLR, are based on minimization of an object function formulated in terms of prescribed (target) pressure distributions. This leaves the user with the problem to translate his design goals in properly defined pressure distributions exhibiting the required aerodynamic characteristics.

Though skilful designers are capable of producing successful designs, as has been demonstrated in sections 2 and 3, the design efficiency can be improved by providing the designer with tools for target pressure specification. To this end two codes have been developed. SAMID (Ref.30) may be used for the selection of spanload distributions leading to minimum induced and viscous drag taking into account aerodynamic, flight-mechanical and structural constraints. CADOS (Ref.31) may be used for selection of appropriate chordwise pressure distributions. The latter code is an interactive optimization system for the solution of minimization (or maximization) problems defined by the user with respect to its object function, design variables and constraints.

SAMID is based on lifting line approximations using the conservation laws of momentum for determination of the induced drag. The viscous drag is approximated for given airfoil characteristics by deriving expressions for the sectional viscous drag in terms of the section lift coefficient using semi-empirical relations and thin airfoil theory. Through variational calculus a set of optimality equations is derived from the object function augmented with constraint terms using Lagrange multipliers. Application of appropriate discretization then leads to a system of linear equations for trailing edge vortex sheet strengths and Lagrange multipliers.

Propeller slipstream interaction with the lifting surfaces may be considered as well as long as it may be assumed that each propeller sheds a helical vortex sheet not influenced by the presence of the wing and confined to a cylindrical stream tube parallel to the free stream direction. The velocity distribution inside the slipstream is assumed to be known. As an example of such an application the results of Fig.4.25 are presented. This figure shows the optimal spanwise circulation distribution for the propeller induced velocity distribution presented in Fig.4.24. Clearly the optimal distribution differs greatly from the "clean wing" distribution. Application of this distribution would restore much of the loss associated with the slipstream swirl.

Using CADOS for chordwise pressure distribution specification implies the definition of a suitable object function and appropriate constraints reflecting the sense in which the target should be optimal. But first of all an appropriate pressure distribution representation should be chosen. Concentrating on transonic flow and pioneering with application of CADOS a number of relatively simple shape functions has been selected leading to a representation as schematically depicted in Fig.4.26. This representation involves a limited number of design variables in the form of coefficients and exponents.

As an example of the practical applicability of CADOS some results may be shown of case studies using the above representation and determining drag by means of boundary layer calculations based on Thwaites method for laminar and Green's lag-entrainment method for turbulent flow.
The first example is a demonstration of the capability to design high lift airfoils. The intention was to maximize lift by changing only the upper surface pressure distribution for a fixed arbitrarily chosen lower surface pressure distribution under the additional constraint that the flow had to remain attached and subsonic everywhere on the airfoil.

Keeping Liebeck's results for the so-called turbulent rooftop in mind, at the first optimization attempt the shape function coefficients were constrained to producing a Stratford type pressure recovery. This resulted in the rooftop solution of Fig.4.27 comparing reasonably well with Liebeck's solution as presented in Ref.32. Application of CADOS with the upper surface pressure distribution entirely free led to a solution with a slightly higher lift coefficient represented by the dashed line in Fig.4.27. To conclude this exercise the NLR airfoil design system of Ref.17 was applied to determine the corresponding geometries. The results are presented in Fig.4.27, showing that the second pressure distribution leads to a somewhat gentler airfoil shape.

The second example that may be presented here concerns transonic low drag design. At first, calculations were performed in order to check the suitability of the shape functions for representation of realistic transonic pressure distributions. To this end CADOS was used to determine the best fit to a pressure distribution calculated by means of the VGK code of Ref.24 for a given airfoil.The result is presented in Fig.4.28 . Apparently the discrepancies are largest in the shock region and at the nose.

Third International Conference on Inverse Design Concepts and Opumization in Engineering Sciences
(ICIDES-III), Editor: G.S. Dulikravich, Washington D.C., October 23-25, 1991.

Subsequently it was attempted to determine a new target pressure distribution aiming at a decrease of the drag with the "best fit" as starting point. Fig.4.29 shows the result, designated "new target". According to the CADOS boundary layer calculations this target should lead to a drag decrease of 5 counts.

Again the NLR airfoil design system was applied for determination of a new airfoil shape, upon which VGK was used for determination of the actual pressure distribution. The latter result is presented in Fig.4.30 in comparison with the original pressure distribution. The discrepancies between the shape function representation and the actual pressure distribution mentioned above may be responsible for the fact that here only 3 counts instead of 5 counts drag decrease is predicted. Nevertheless, the present example may be considered as illustrating the usefulness of CADOS in transonic airfoil design.

5.CONCLUDING REMARKS

A survey has been given of contemporary practice of aerodynamic design in The Netherlands, focusing on airfoil and wing design. It will have become clear that the application of analysis and design codes has become common practice in aerodynamic aircraft design procedures.

As has been mentioned before, work is in progress at NLR to extend the design system for wings in subsonic flow for application to wings of wing-body combinations in viscous transonic flow. A somewhat longer term development is the extension of this system to application for multi-point wing design. This work has been started within a BRITE/EURAM project sponsored by the European Community and aims at the development of a method for the design of wings in transonic flow, such that at a number of different flow conditions the wing (without changing the geometry) will operate according to preset requirements.

6.REFERENCES

1.Obert,E.:'The aerodynamic development of the Fokker 100',ICAS-88-1.6.2,1988

2.Voogt,N.,Mol,W.J.A.,Stout,J.,Volkers,D.F.:'CFD applications in design and analysis of the Fokker 50 and Fokker 100.',Validation of Computational Fluid Dynamics, Lissabon, 1988

3.Fray,J.M.J., Slooff,J.W.:'a constrained inverse method for the aerodynamic design of thick wings with given pressure distribution in subsonic flow',AGARD CP No.285,paper 16,1980

4.Slooff,J.W., Voogt,N.:'Aerodynamic design of thick,supercritical wings through the concept of equivalent subsonic pressure distribution',NLR MP 78011 U,1978

5.Jameson,A., Caughey,D.A.:'Numerical calculations of transonic flow past a swept wing',ERDA Report COO-3077-140, Courant Institute of Mathematical Sciences, New York University,1977

6.van der Vooren,J., van der Kolk,J.Th., Slooff,J.W.:'A system for the numerical simulation of sub- and transonic viscous attached flows around wing-body configurations',AIAA paper 82-0935,NLR MP 82019 U,1982

7.Labrujère,Th.E., Loeve,W., Slooff,J.W.:'An approximate method for the calculation of the pressure distribution on wing-body combinations at subcritical speeds',AGARD CP No.71,paper 11,NLR MP 70014 U,1970

8.Labrujère,Th.E., Sytsma,H.A.:'Aerodynamic interference between aircraft components ; illustration of the possibility for prediction',NLR MP 72020 U,1972

9.Lindhout,J.P ., de Boer,E., van den Berg,B.:'A method for the calculation of 3D boundary layers on practical wing configurations',NLR MP 79003 U,1979

10.Boermans,L.M.M., Waibel,G.:'Aerodynamic and structural design of the standard class sailplane ASW-24',ICAS-88-2.7.2,1988

11.Boermans,L.M.M.: Private communication, 1991

12.van Ingen,J.L.:'Advanced computer technology in aerodynamics: a program for airfoil section design utilizing computer graphics',AGARD Lecture Series no.37, 1970

13.van Ingen,J.L., Boermans,L.M.M., Blom,J.J.H.:'Low speed airfoil section research at Delft University of Technology',ICAS-80-10.1,1980

14.Timman,R.:'The direct and inverse problem of airfoil theory. A method to obtain numerical solutions', NLL-F16,1951

15.van Ingen,J.L.:'A suggested semi-empirical method for the calculation of the boundary layer transition region', Delft University of Technology, Faculty of Aerospace Engineering, VTH-74, 1956

16.Slooff,J.W.:' A survey of computational methods for subsonic and transonic aerodynamic design', NLR MP 84066 U, ICIDES ,1984

17.Labrujère,Th.E.:'MAD : A system for computer aided analysis and design of multi-element airfoils", NLR TR 83136 L, 1983

18.Oskam,B.:'A calculation method for the viscous flow around multi-component airfoils', NLR TR 79097 U, 1979

19.van Egmond,J.A., van den Berg,B., Labrujère,Th.E.:' Application of a constrained inverse method in the aerodynamic design of a low-speed wing-slat configuration', NLR TR 83123 L, 1983

20.van Egmond,J.A., van den Berg,B.:' Design of an airfoil leading edge slat using an inverse aerodynamic calculation method', AGARD CP-365 paper 6-1, 1984

21.Rozendal,D.:'Design of a thick natural laminar flow airfoil for a Mach number of .65', NLR Memorandum AX-91-004, 1991

22.Piers,W.J., van Egmond,J.A., Houwink,R.:'Aerodynamic design of the NLR/VSH 8801 airfoil for application in a wind turbine blade (in Dutch)', NLR TR 88070 C, 1988

23.Bauer,F., Garabedian,P., Korn,D.:'Supercritical wing sections',Lecture notes in economics and mathematical systems.Vol.66,Springer Verlag,Berlin,1972

24.Collyer,M.R.:'An extension to the method of Garabedian and Korn for the calculation of transonic flow past an airfoil to include the effects of a boundary layer and wake',RAE TR77104,1977

25.Fray,J.M.J, Slooff,J.W., Boerstoel,J.W., Kassies,A.:' Design of transonic airfoils with given pressure, subject to geometric constraints', NLR TR 84064, 1984

26.Fray,J.M.J, Slooff,J.W., Boerstoel,J.W., Kassies,A.:' Inverse method with geometry constraints for transonic airfoil design ', NLR MP 84069 U, ICIDES, 1984

27.Brandsma,F.J., Fray,J.M.J.:'A system for transonic wing design with geometric constraints based on an inverse method', NLR TP 89179 L, 1989

28.Van der Vooren,J., van der Wees,A.J., Meelker,J.H.:'MATRICS, Transonic potential flow calculations about transport aircraft', AGARD Conf.Proc. No. 412,1986

29.Van der Wees,A.J.:' FAS multigrid employing ILU-SIP smoothing: a robust fast solver for 3D transonic potential flow', NLR MP 85072 U, 1985, Lecture Notes in Mathematics 1228, Springer Berlin,1986

30.Van den Dam,R.F.:'Constrained spanload optimization for minimum drag of multi-lifting-surface configurations',AGARD CP No.463, Paper 16, 1989

31.Van Egmond,J.A.:'Numerical optimization of target pressure distributions for subsonic and transonic airfoil design',AGARD-CP No.463, Paper 1, 1989

32.Smith,A.M.O.:'High lift aerodynamics', AIAA paper No.74-939,1974

TABLE I : The Fokker 100 wing development (Ref.1)

Wing 1 : The basic F-28 wing, defined by four wing sections connected with straight generators
Wing 3 : Wing 1 with 0.75 m span extension (defining section V)
Wing 4 : Wing 1 modified with :
- forward extension of the chords of sections I,II and III
- modification of the front part of sections I and II
- 1.5 m span extension

Wing 5 : Wing 1 modified with :
- 1.5 % chord extension and modified front part of section IV
- straight leading edge at outer wing defined by section II and IV
- 5 % chord extension of section I
- 1.5 m span extension

Wing 6 : As wing 5 but with 9% chord extension of section I
Wing 8 : Wing 5 modified with rearward chord extension and rear camber
Wing 10: Wing 8 modified with :
- 0.75 m span extension
- straight leading edge between section III and V leading to kinks at sections II and III
- new front part of section IV

Wing 11: Wing 10 modified with :
- new lower leading edge of sections III and IV

Wing 12: Wing 11 modified with :
- new leading edge of section II

Third International Conference on Inverse Design Concepts and Optimization in Engineering Sciences
(ICIDES-III),Editor:G.S.Dulikravich, Washington D.C.,October 23-25,1991

Fig. 1.1 Fokker 100 prototype - ref. 4

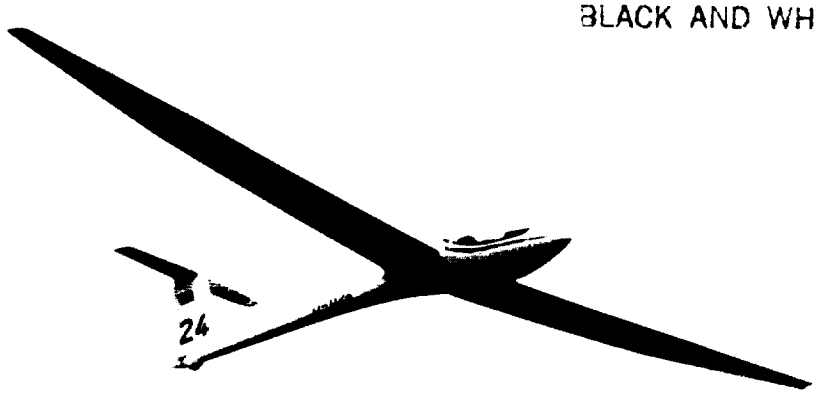

Fig. 1.2 ASW-24. ref. 11

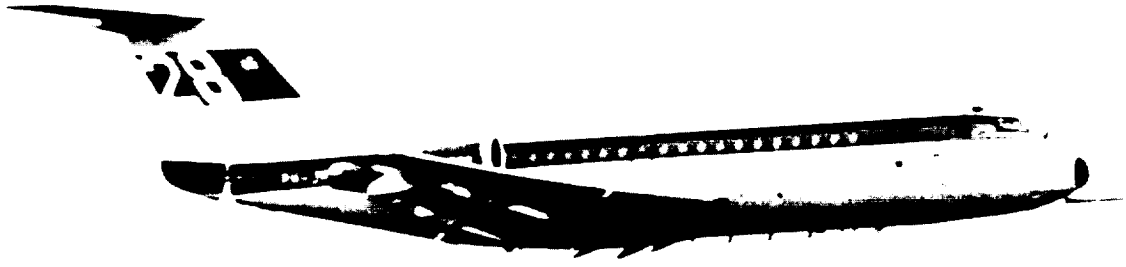

Fig. 1.3 Fokker F-28

Third International Conference on Inverse Design Concepts and Optimization in Engineering Sciences
(ICIDES-III) Editor:C.S.Dulikravich Washington D.C. October 23-25,199

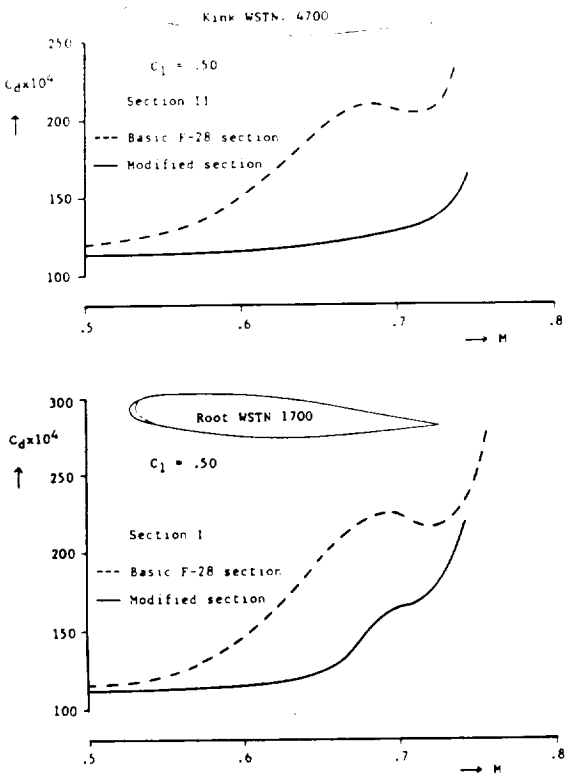

Fig. 2.1 Effect of modifications to root and kink sections of the F-28 wing. ref. 1

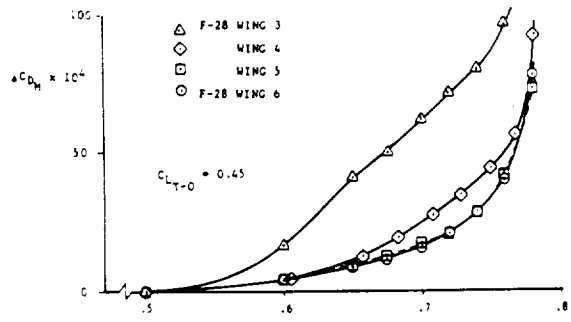

Fig. 2.2 Mach drag rise characteristics of wings 3, 4, 5 and 6 at CLT-O = 0.45. ref. 1

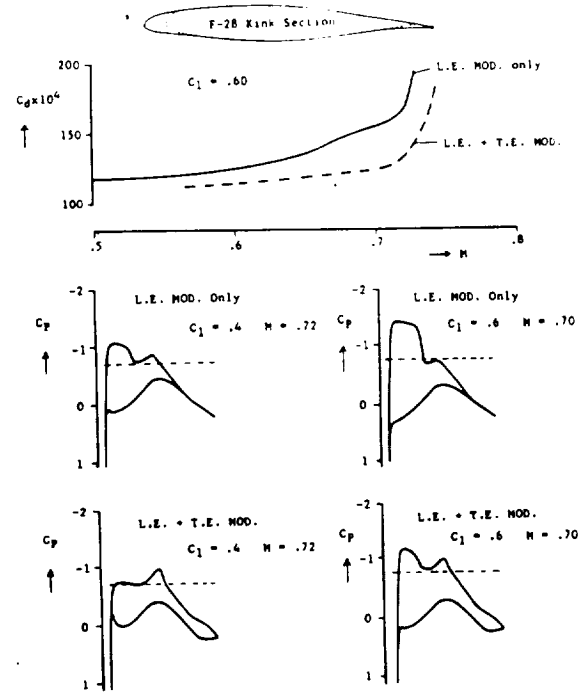

Fig. 2.3 Effect of trailing-edge modification on Mach-drag rise and pressure distribution. ref. 1

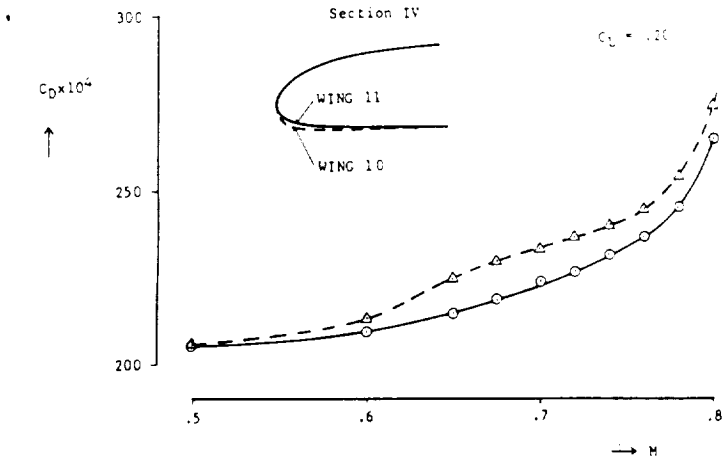

Fig. 2.4 Effect of blunt leading-edge on the Mach-drag rise at low lift coefficient. ref. 1

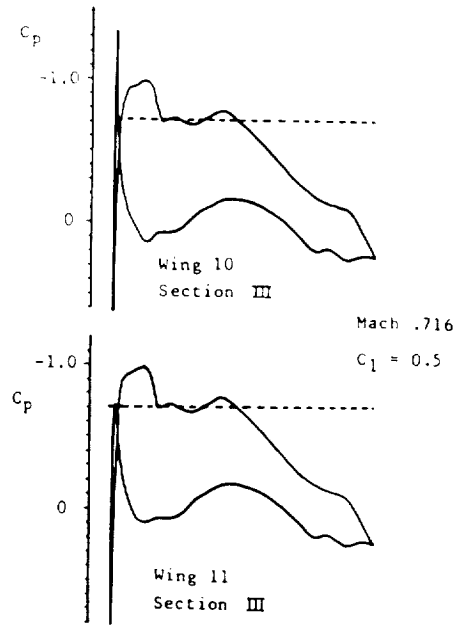

Fig. 2.5 Effect of blunt leading-edge on the lower-surface leading-edge suction peak. ref. 1

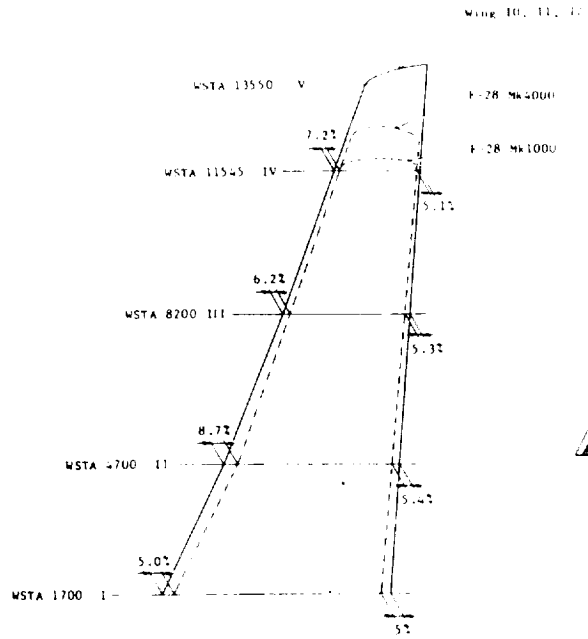

Fig. 2.6 a Comparison between F-28 and Fokker 100 wing geometry. ref. 1

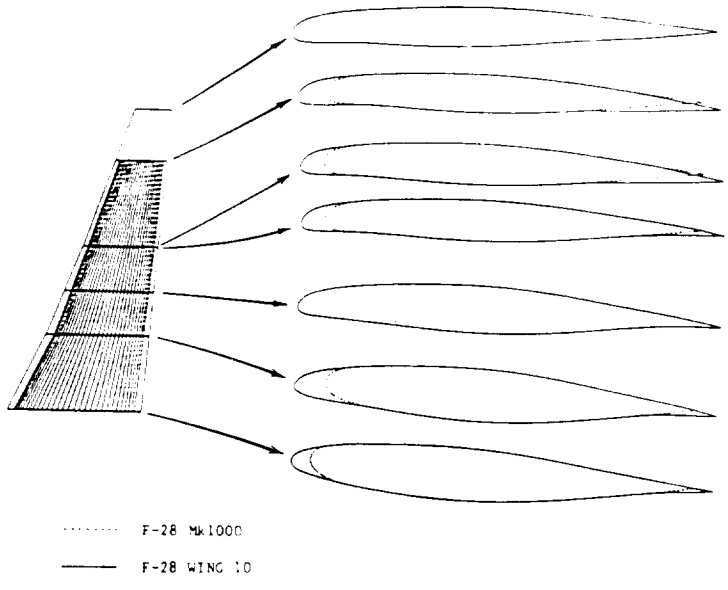

Fig. 2.6 b

Third International Conference on Inverse Design Concepts and Optimization in Engineering Sciences (ICIDES-III), Editor: G.S.Dulikravich, Washington D.C. October 23-25,1991

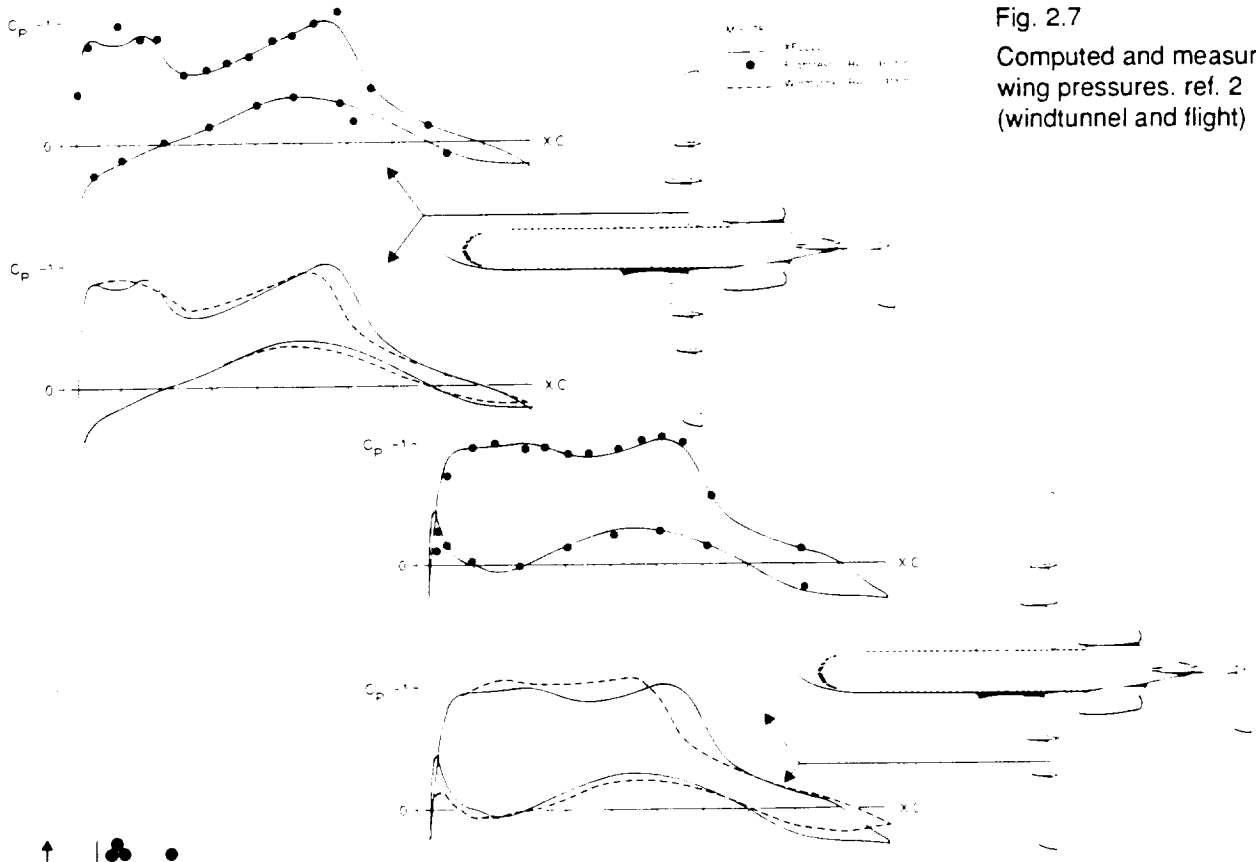

Fig. 2.7
Computed and measured wing pressures. ref. 2 (windtunnel and flight)

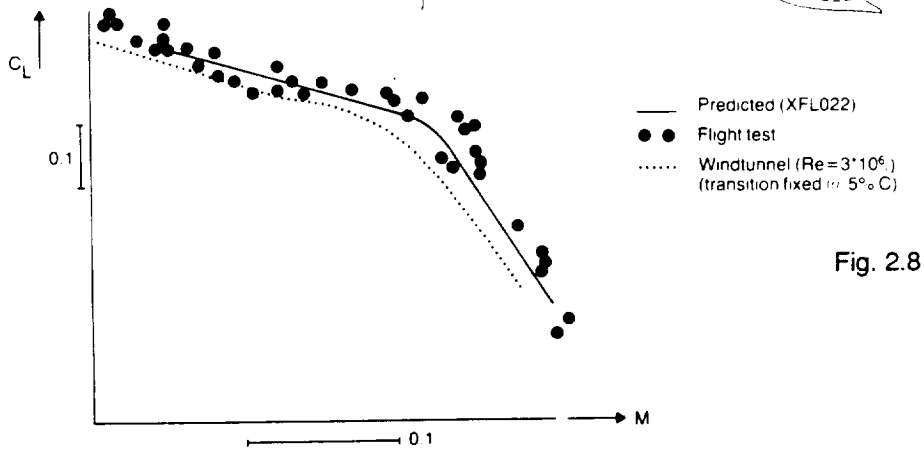

Fig. 2.8 Comparison of buffet onset boundaries. ref. 2

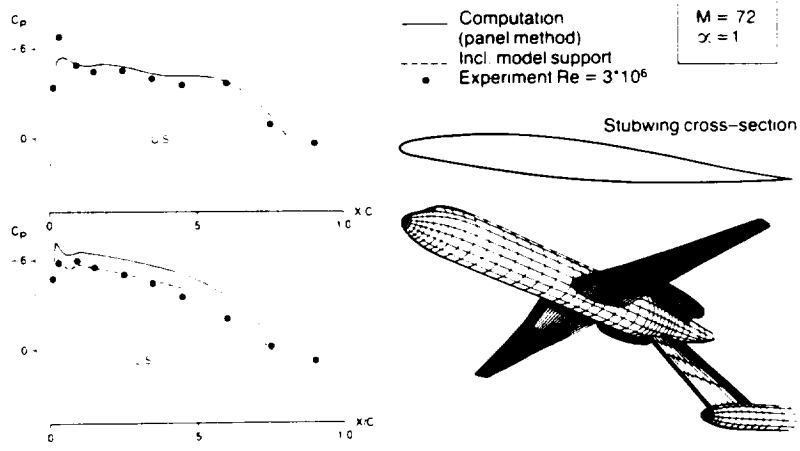

Fig. 2.9
Computed and measured stubwing pressures. ref. 2

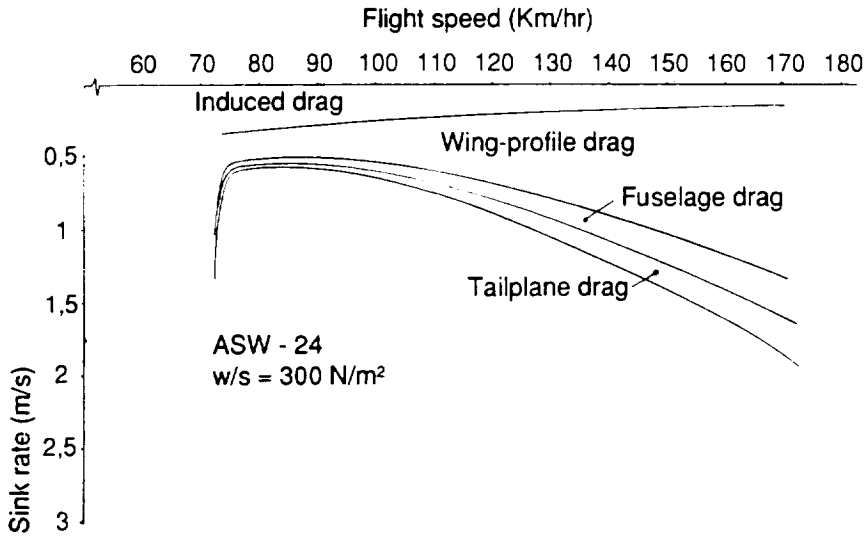

Fig. 3.1 Flight performance polar of ASW-24 ref. 11

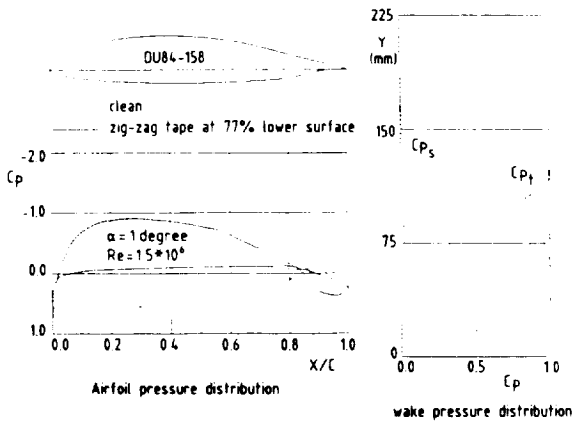

Fig. 3.2 Measured airfoil and wake pressure distributions. ref. 10

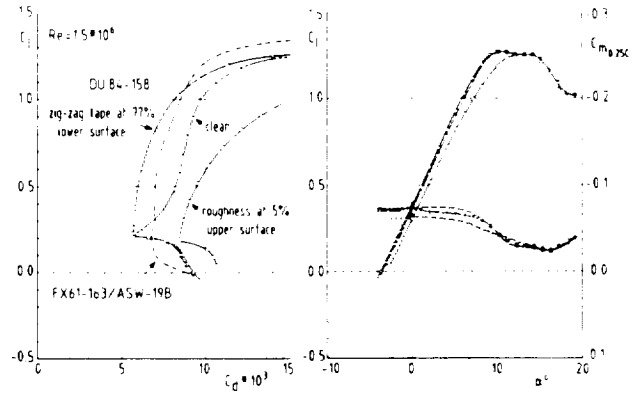

Fig. 3.3 Measured aerodynamic characteristics. ref. 10

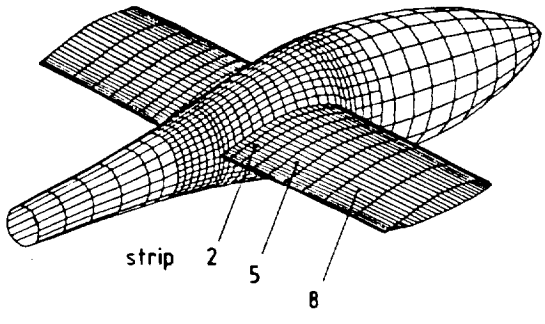

Fig. 3.4 Part of panel scheme of ASW-24 wing-fuselage combination. ref. 10

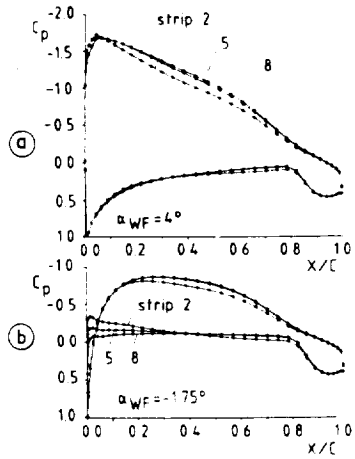

Fig. 3.5 Pressure distributions of wing strips in the wing root area. ref. 10

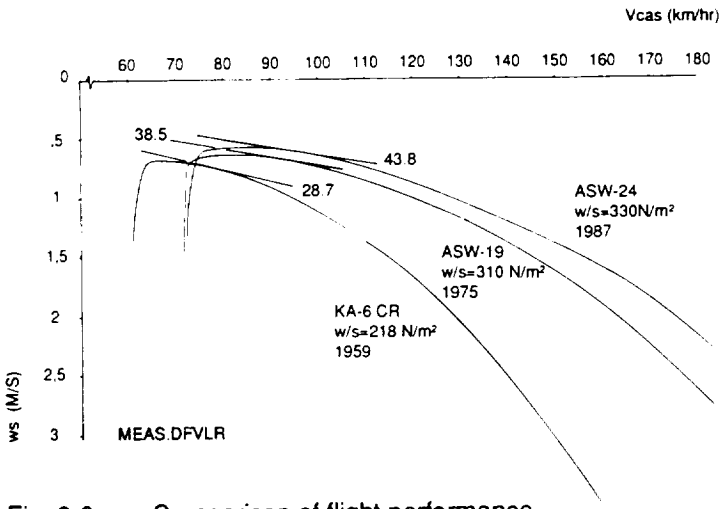

Fig. 3.6 Comparison of flight performance polars. ref. 11

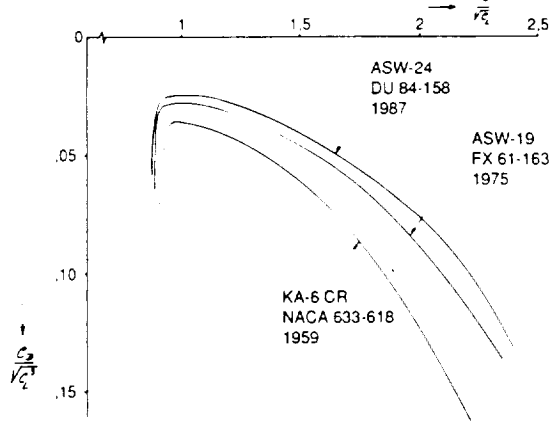

Fig. 3.7 Comparison of aerodynamic quality. ref. 11

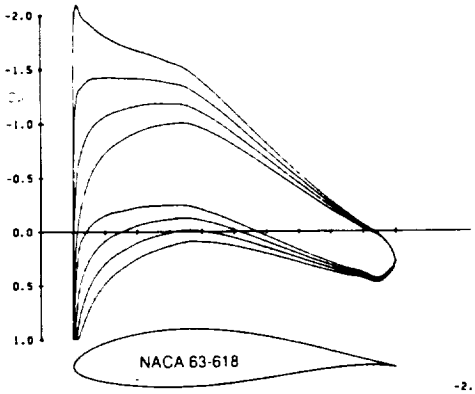

Fig. 3.8 a

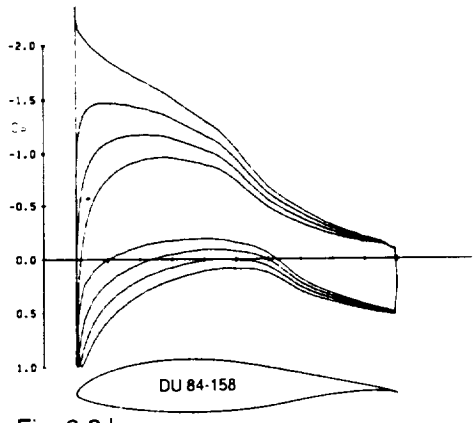

Fig. 3.8 b

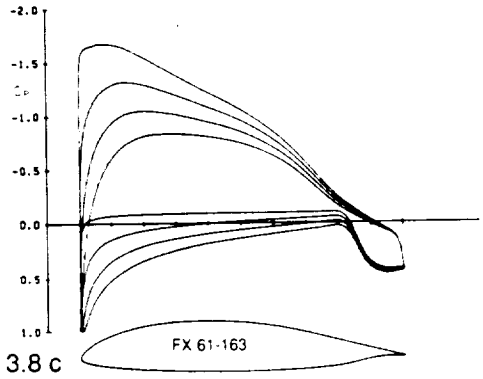

Fig. 3.8 c

Fig. 3.8 Comparison of pressure distribution ref. 11

Third International Conference on Inverse Design Concepts and Optimization in Engineering Sciences
(ICIDES-III), Editor: G.S.Dulikravich, Washington D.C., October 23-25,1991

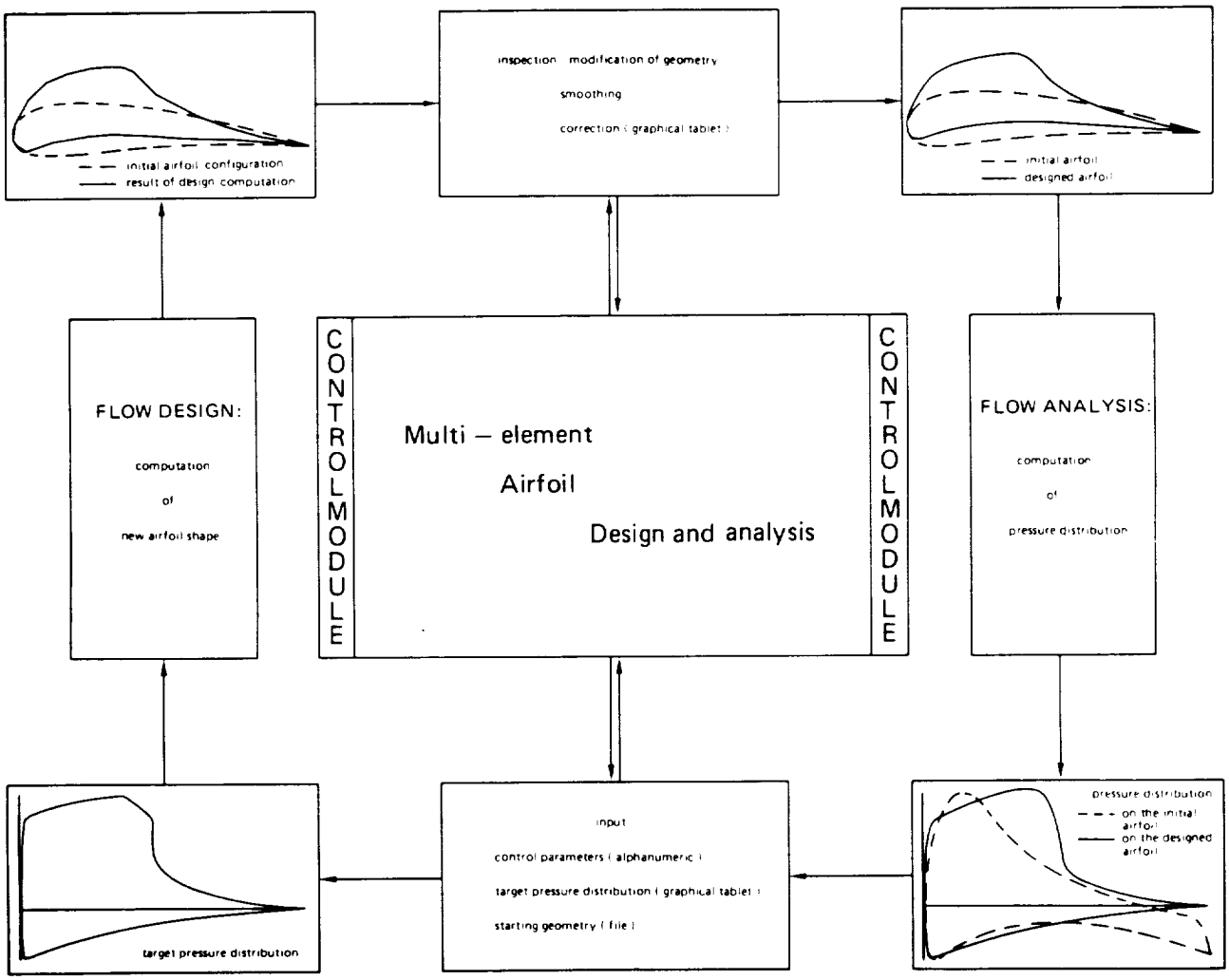

Fig. 4.1 ref. 17

Fig. 4.2 Sketch of the original wing-slat configuration. ref. 19

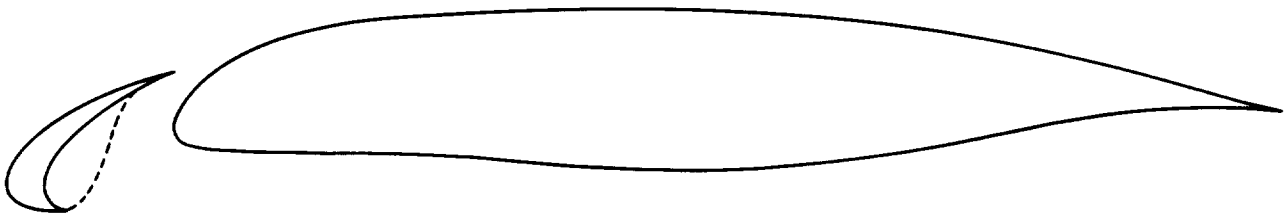

(SLAT POSITION : OV = 0
GA = 0.025
DS = 10°)

----- BUBBLE SIMULATION ; USED IN COMPUTATIONS

Third International Conference on Inverse Design Concepts and Optimization in Engineering Sciences (ICIDES-III), Editor: G.S. Dulikravich, Washington D.C. October 23-25, 1991

$\alpha = 20.16°$ Rec = 3.1×10^6
OV = 0 GA = 2.5 % DS = 10°

Fig. 4.3 Measured pressure distribution; original wing-slat configuration α=20.2 $C\ell$ =2.13. ref.19

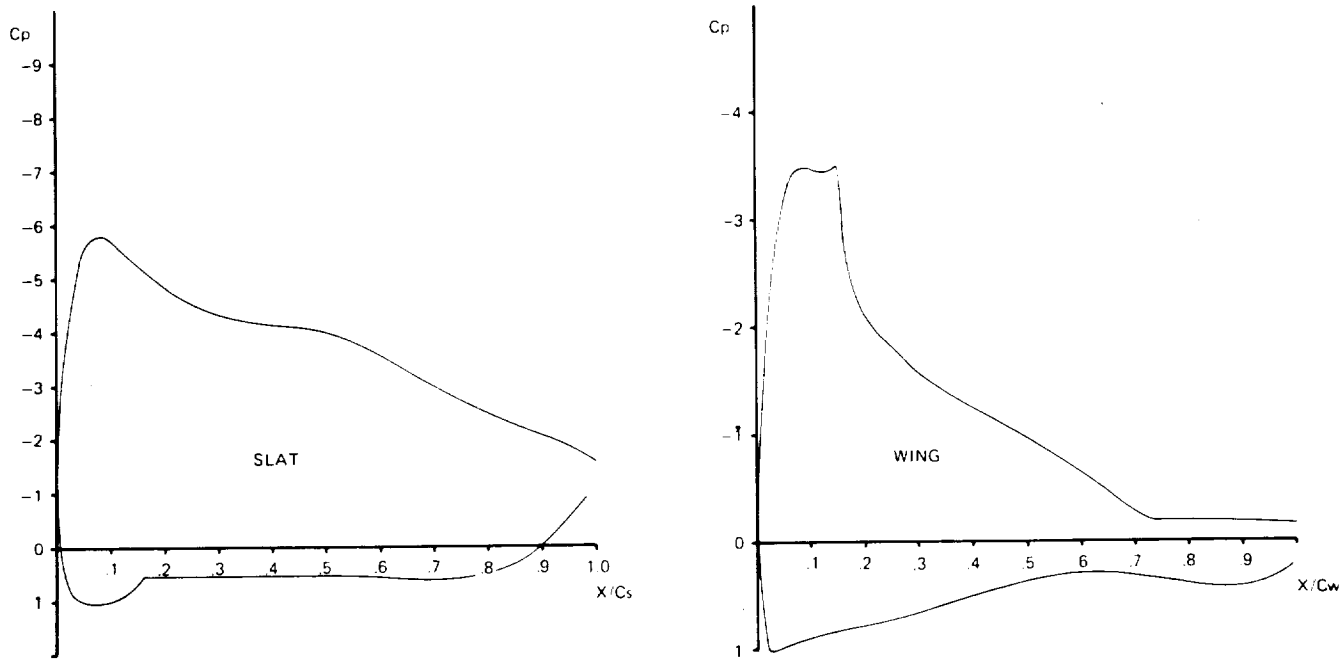

TARGET PRESSURE DISTRIBUTION
ORIGINAL " "
EXPERIMENTAL PRESSURE DISTRIBUTION ON SLAT LOWER SURFACE
} POTENTIAL FLOW (MAD)

Fig. 4.4 Target pressure distribution for new wing-slat configuration α=17°. ref. 19

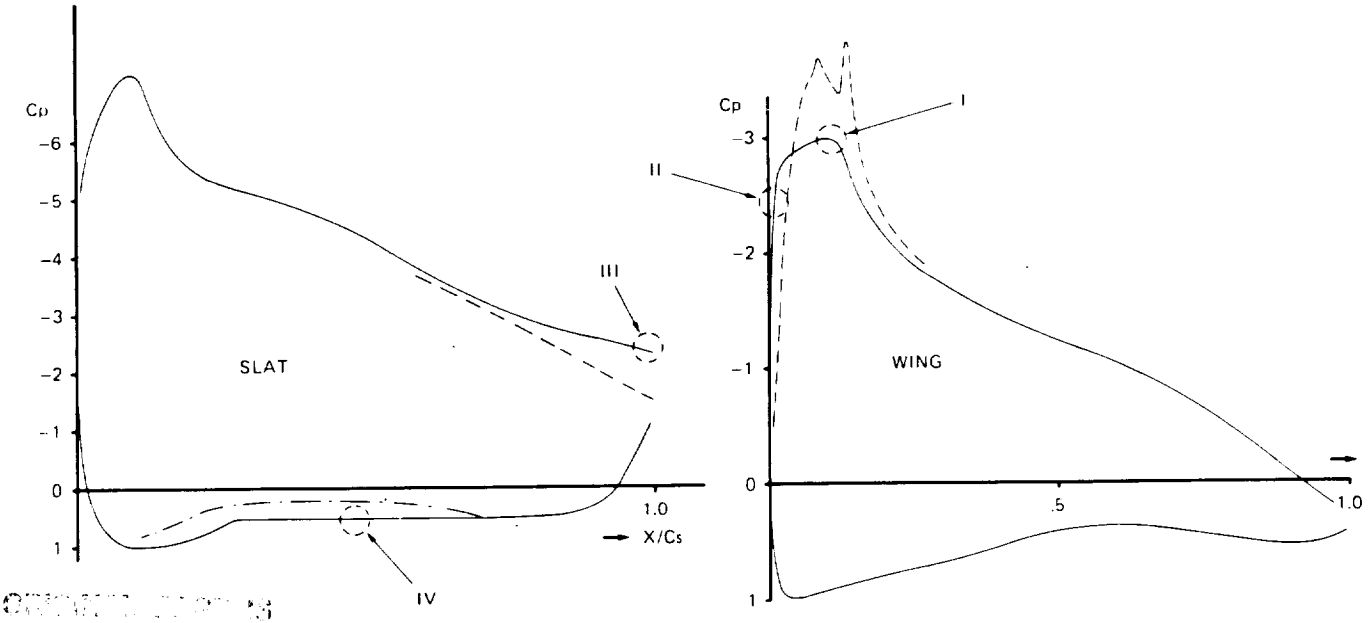

Third International Conference on Inverse Design Concepts and Optimization in Engineering Sciences (ICIDES-III), Edgar C.S. Dulikravich, Washington D.C. October 23-25, 1991

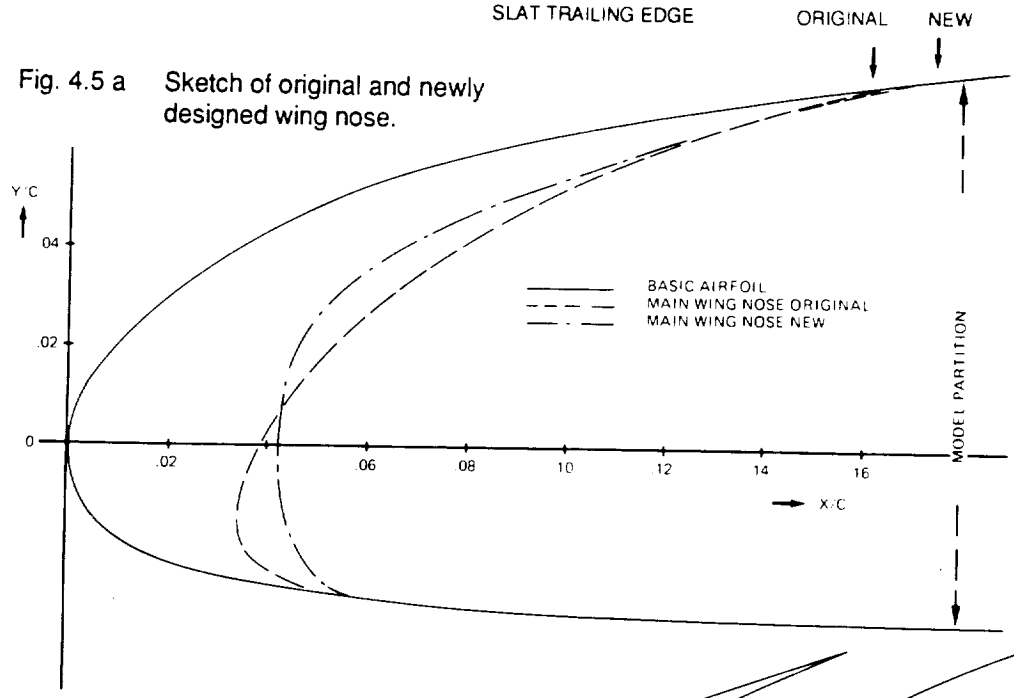

Fig. 4.5 a Sketch of original and newly designed wing nose.

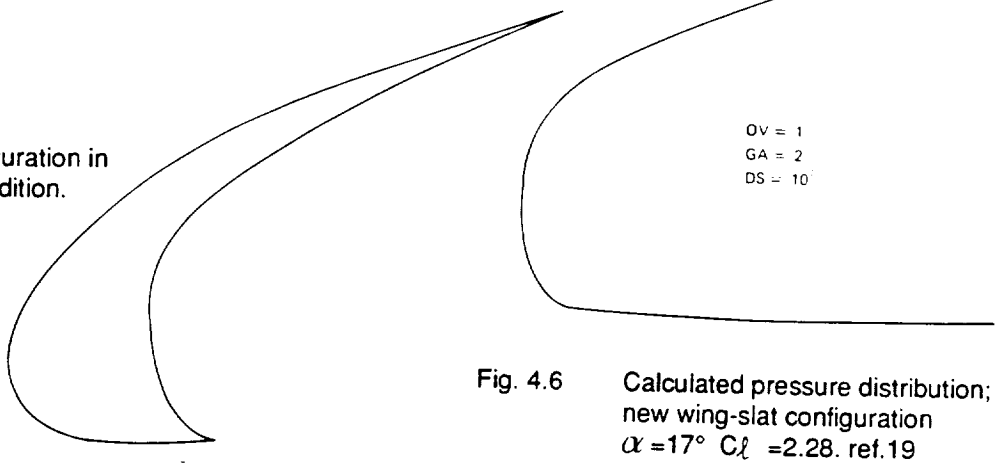

Fig. 4.5 b
Sketch of the new configuration in experimental design condition.

Fig. 4.6 Calculated pressure distribution; new wing-slat configuration α =17° $C\ell$ =2.28. ref.19

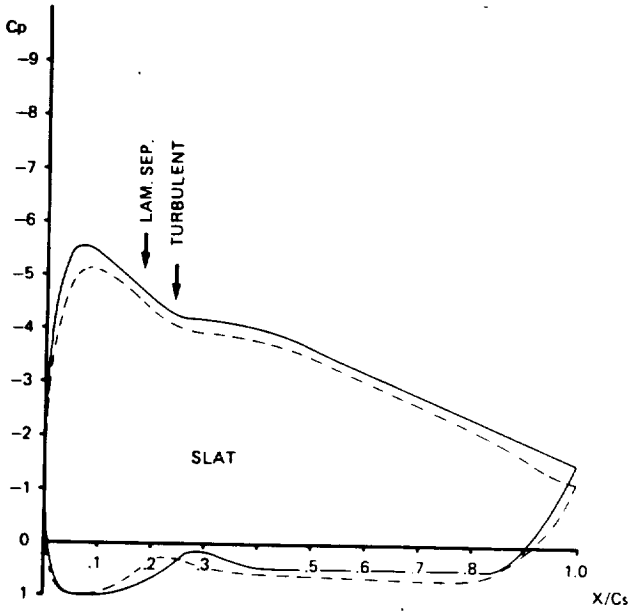

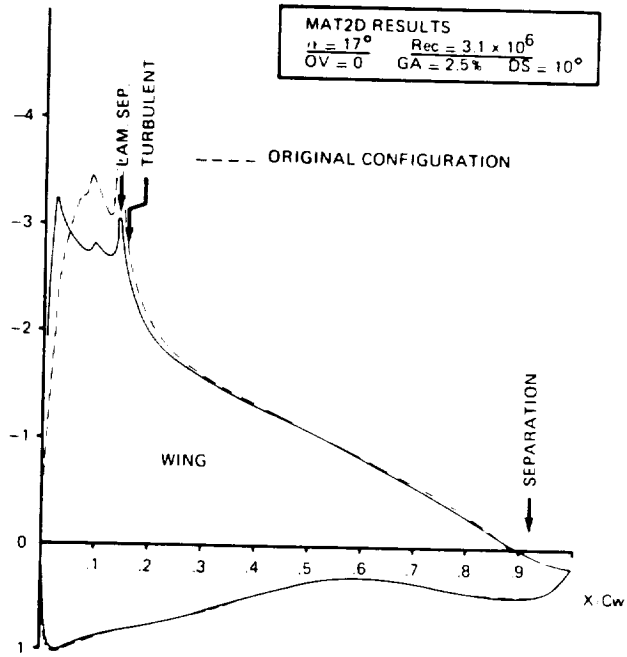

Third International Conference on Inverse Design Concepts and Optimization in Engineering Sciences (ICIDES-III) Editor C.S.Dulikravich, Washington D.C. October 23-25,1991

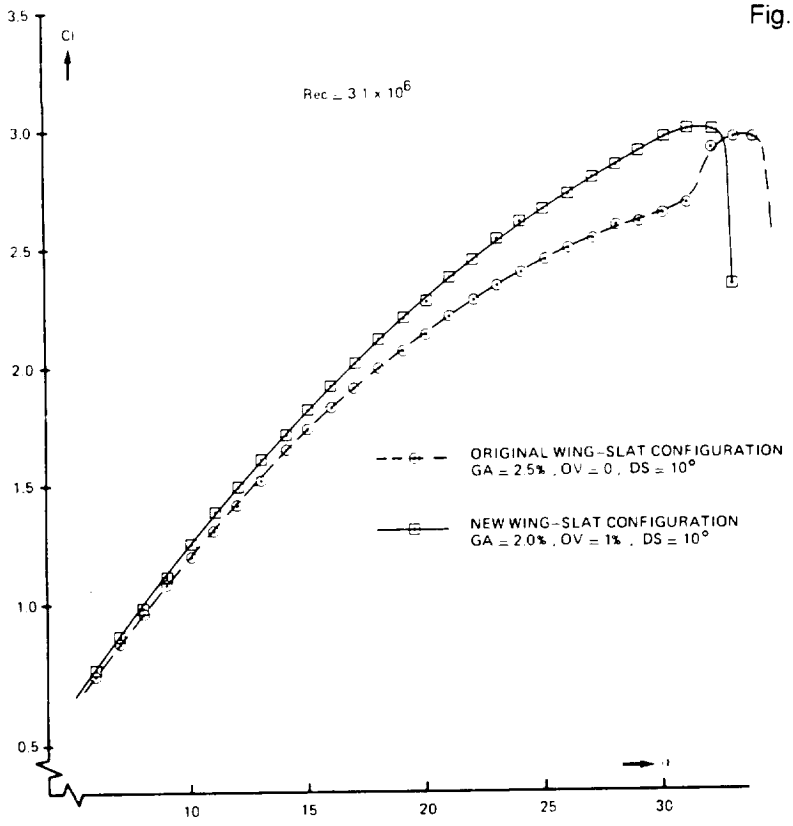

Fig. 4.7 Measured $C\ell$ - α curves for both wing-slat configurations. ref 19

Fig. 4.8 Measured $C\ell$ -Cd curves for both wing-slat configurations. ref. 19

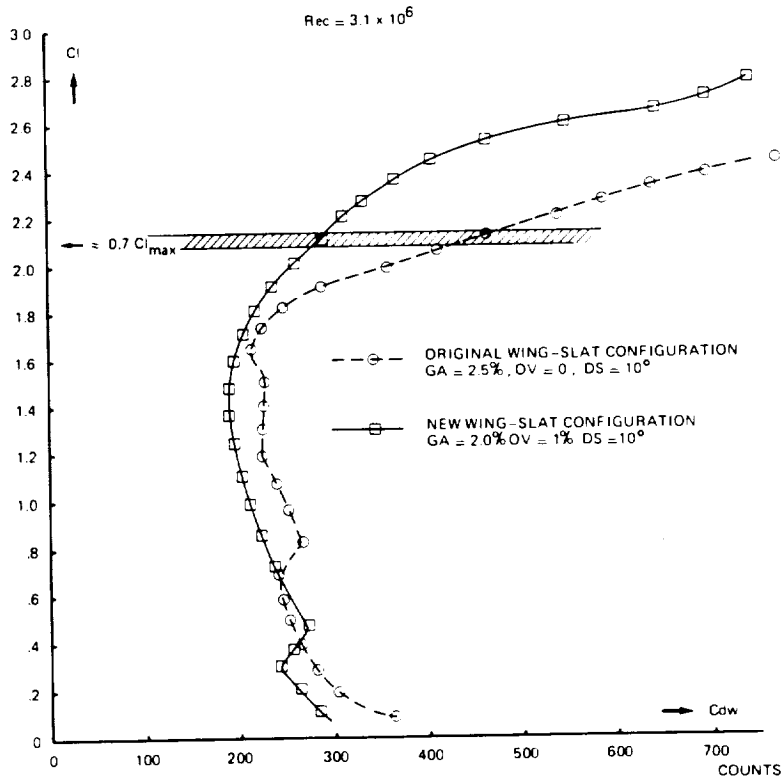

Third International Conference on Inverse Design Concepts and Optimization in Engineering Sciences
(ICIDES-III) Editor:G.S.Dulikravich Washington D.C. October 23-25,1991

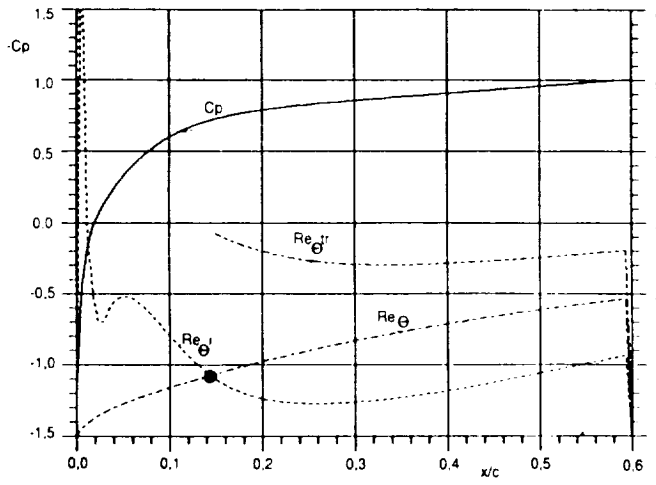

Fig. 4.9 Upper side target. ref.21

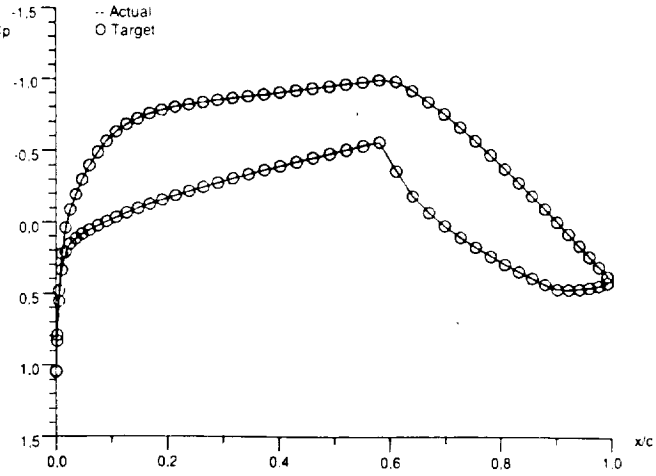

Fig. 4.10 Actual and target pressure distribution. ref. 21

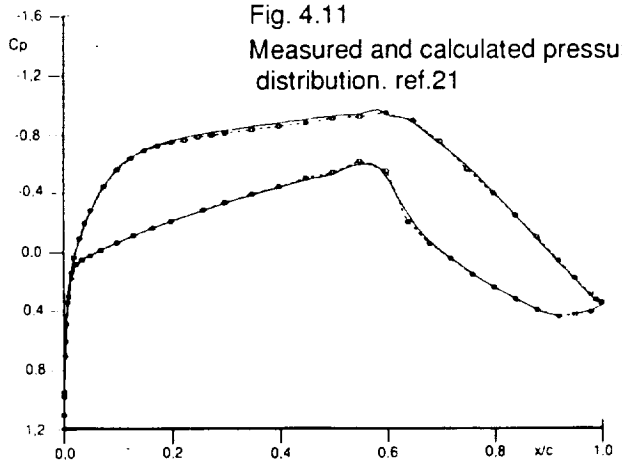

Fig. 4.11
Measured and calculated pressure distribution. ref.21

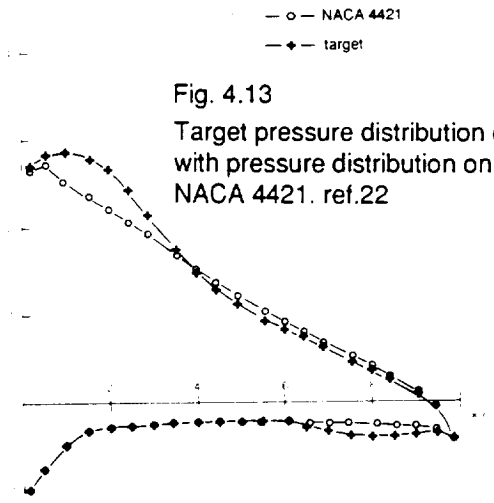

Fig. 4.13
Target pressure distribution compared with pressure distribution on NACA 4421. ref.22

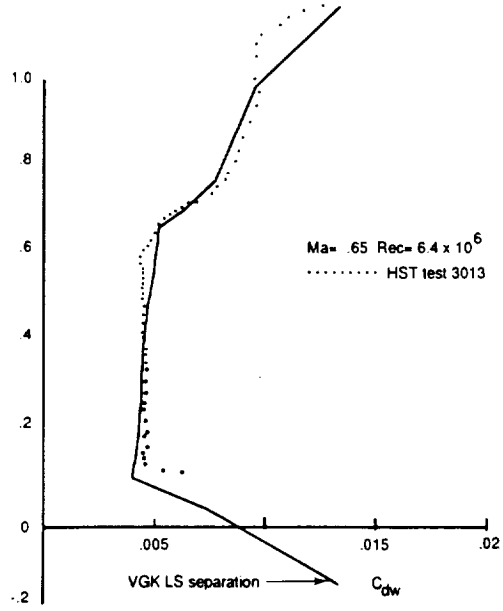

Fig. 4.12 Comparison of experimental and theoretical Cℓ -Cd curves for the design Mach number. ref. 21

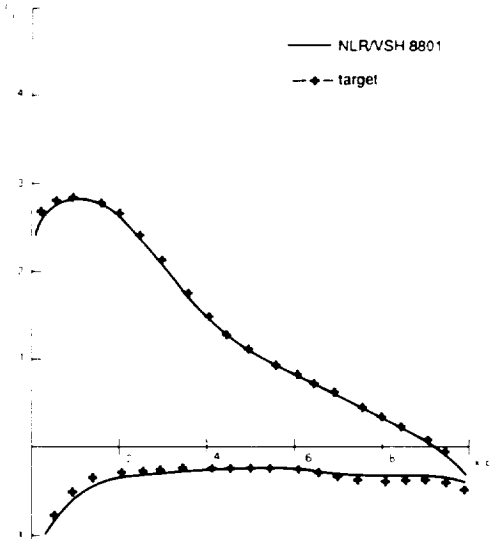

Fig. 4.14 Actual and target pressure distribution. ref. 22

Third International Conference on Inverse Design Concepts and Optimization in Engineering Sciences
(ICIDES-III), Editor: G.S. Dulikravich, Washington D.C., October 23-25, 1991

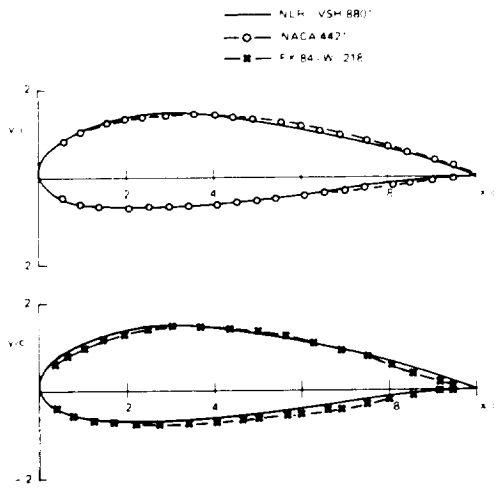

Fig. 4.15 Comparison of airfoil shapes. ref. 22

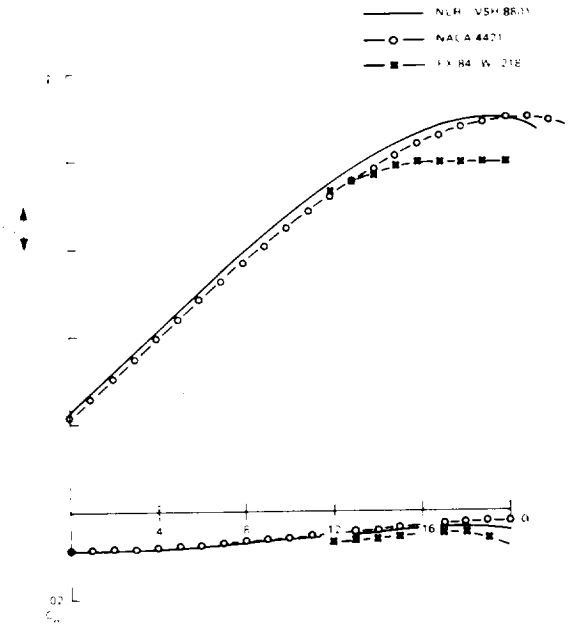

Fig. 4.16 Calculated lift and moment coefficient (Re=3 x 10^6). ref.22

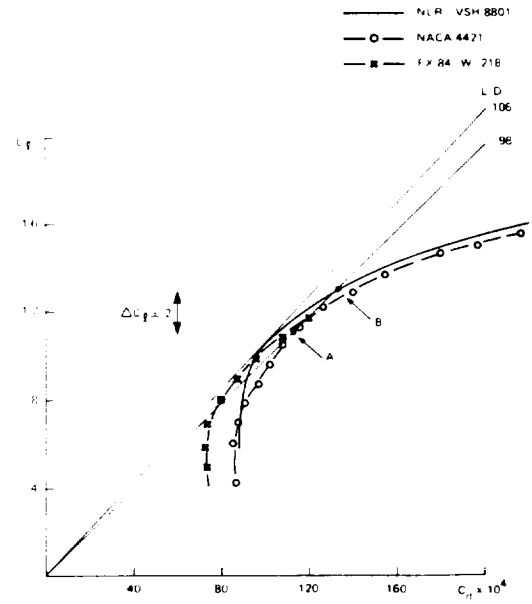

Fig. 4.17 Calculated Cℓ -C d curves (Re = 3 x 10 6). ref. 22

a) Wing platform and top view of body

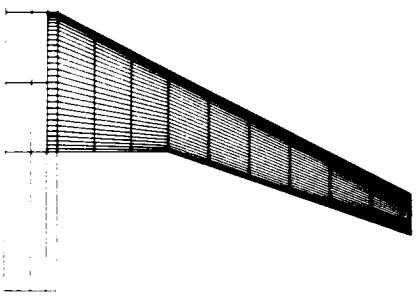

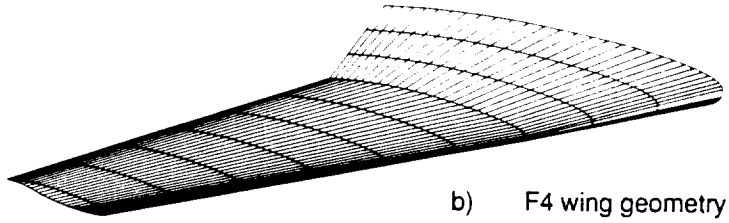

b) F4 wing geometry

Fig. 4.18 F4 wing attached to pencil shaped body used as an example. ref. 27

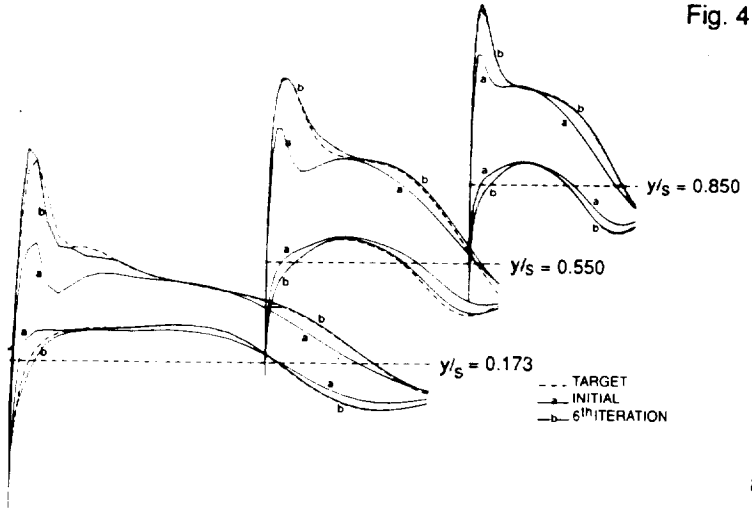

Fig. 4.19 Results of F4 wing reconstruction with influence of body for M=0.75 and 0°. (the target corresponds to the original geometry of fig. 4.18). ref. 27

a) Results for the pressure distribution at three spanwise stations (near root, near midspan near tip).

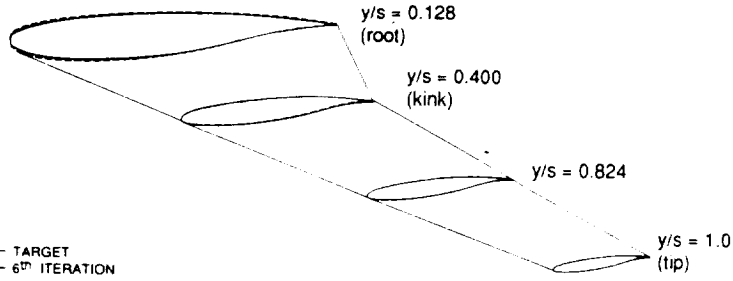

b) Results for the geometry at four spanwise stations

Third International Conference on Inverse Design Concepts and Optimization in Engineering Sciences
(ICIDES-III), Editor: G.S. Dulikravich, Washington D.C. October 23-25, 1991

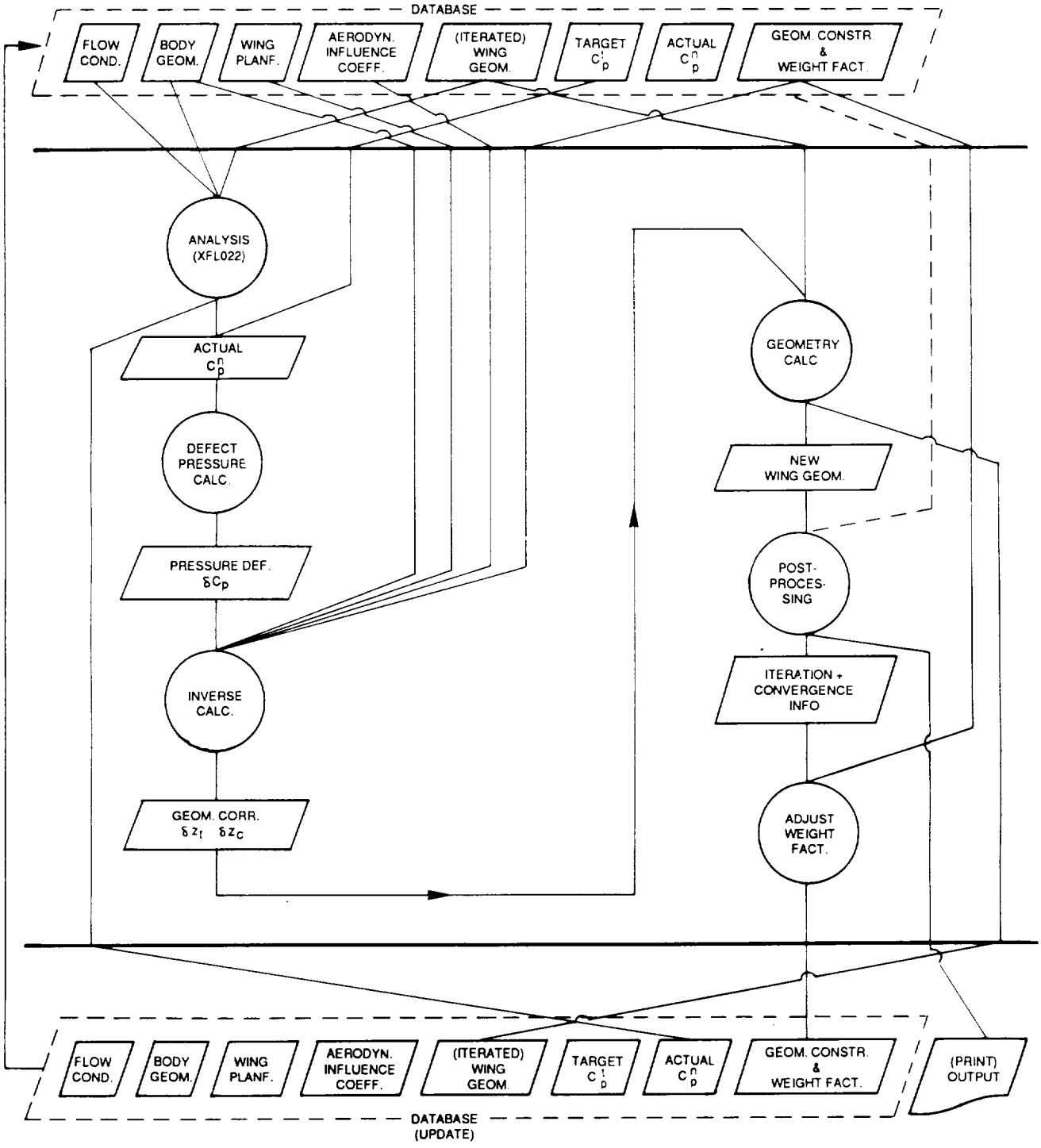

Fig. 4.20 Functional breakdown of the design procedure. ref. 27

Third International Conference on Inverse Design Concepts and Optimization in Engineering Sciences
(ICIDES-III), Editor: G.S. Dulikravich, Washington D.C., October 23-25, 199

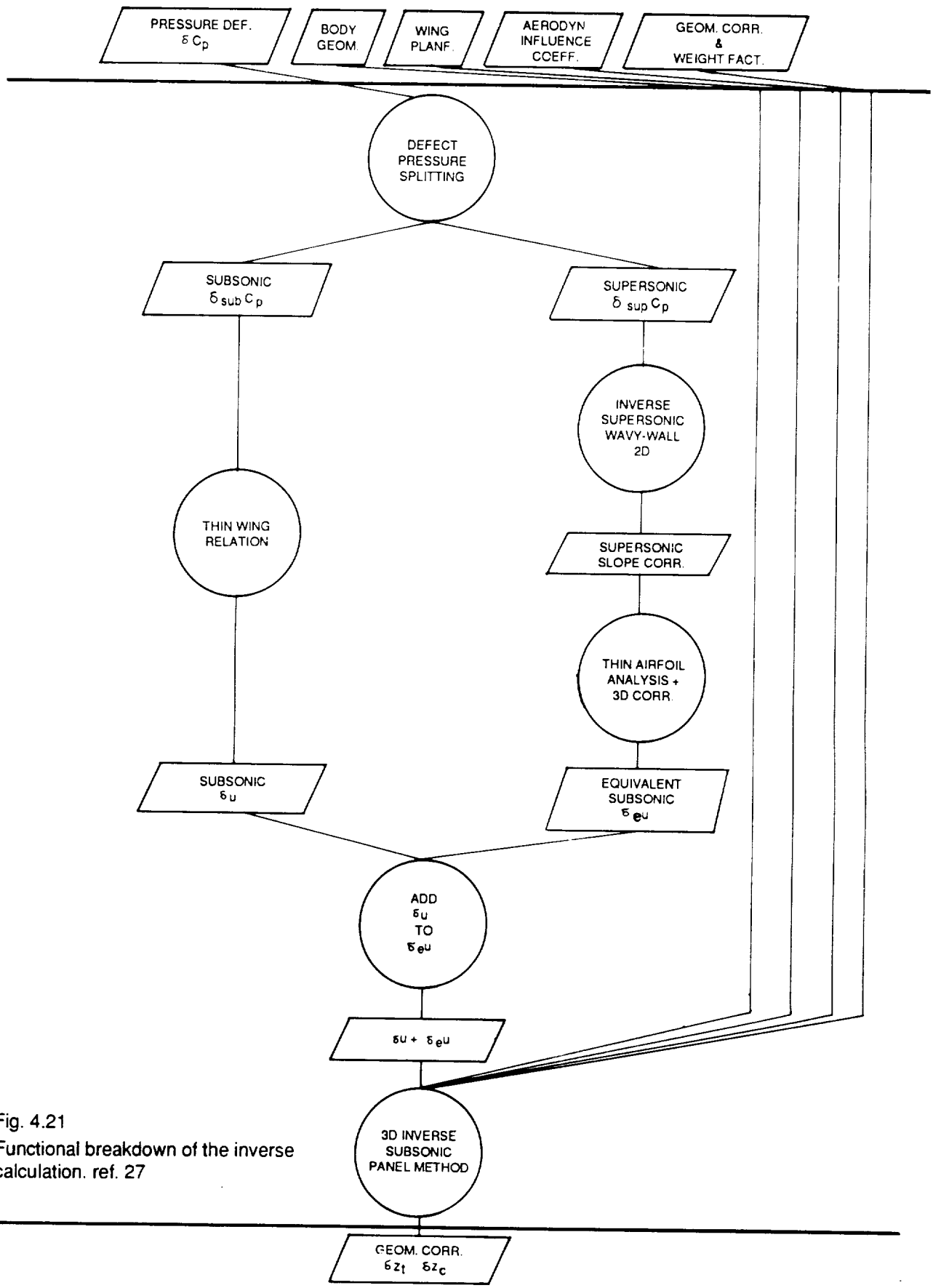

Fig. 4.21
Functional breakdown of the inverse calculation. ref. 27

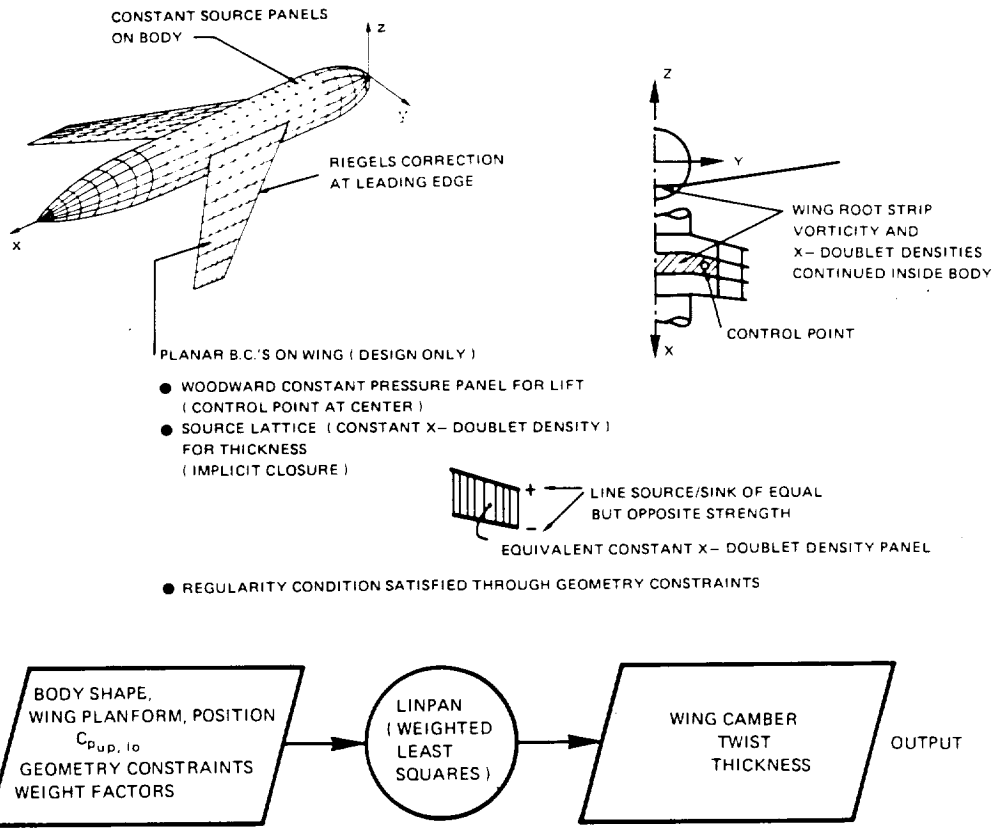

Fig. 4.23 NLR linear subsonic inverse code. ref. 30

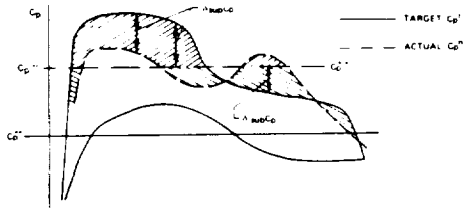

Fig. 4.22 Defect pressure split. ref. 27

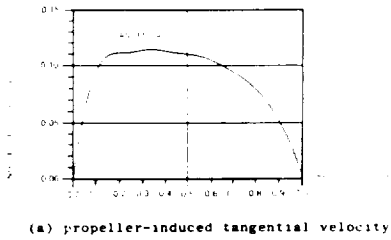

(a) propeller-induced tangential velocity

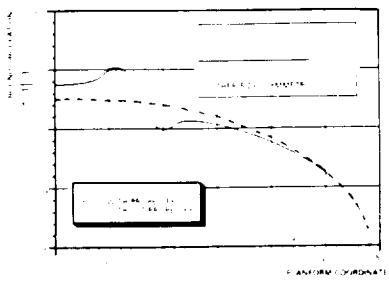

Fig. 4.25 Optimal bound circulation distribution for a wing with two up-inboard rotating propellors. ref. 30

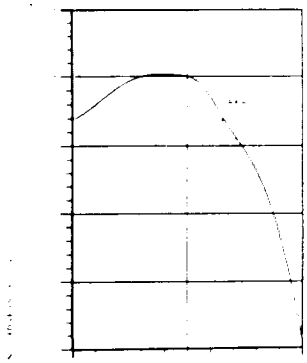

b) Propellor-induced axial velocity.

Fig. 4.24 Propellor- induced velocities. ref 30

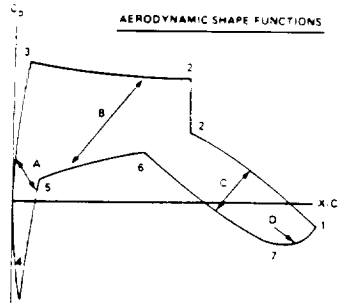

Fig. 4.26 Aerodynamic shape functions. ref. 31

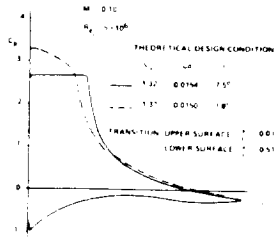

Fig. 4.27 High lift solutions. ref. 31

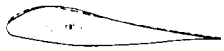

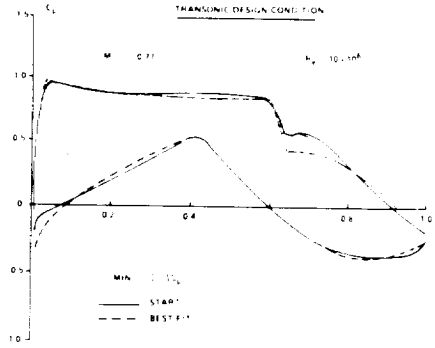

Fig. 4.28 Transonic design condition. ref. 31

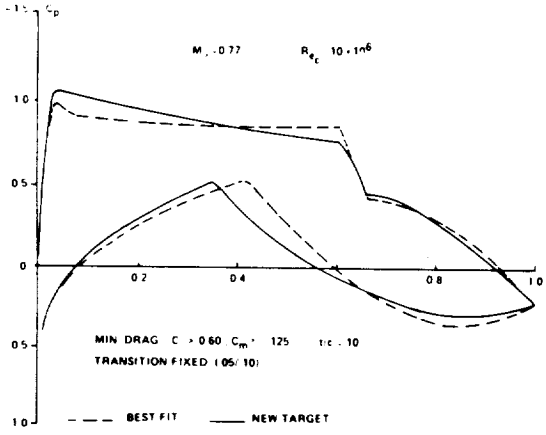

Fig. 4.29 Transonic design condition. ref 31

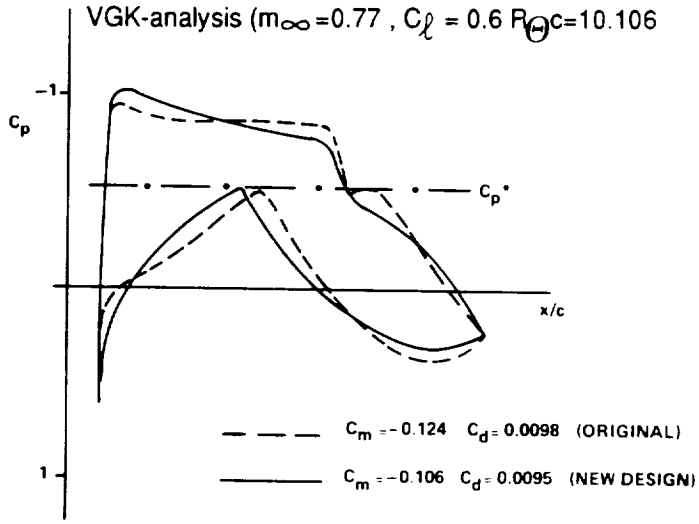

Fig. 4.30 Transonic design condition. ref. 31